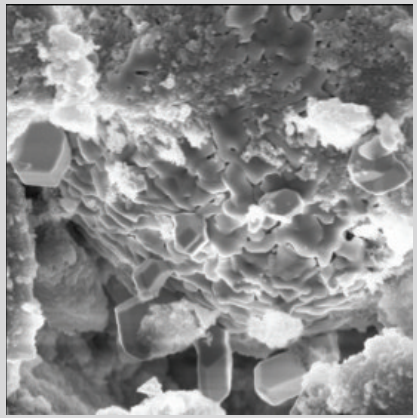
Karlsruhe Institute of Technology

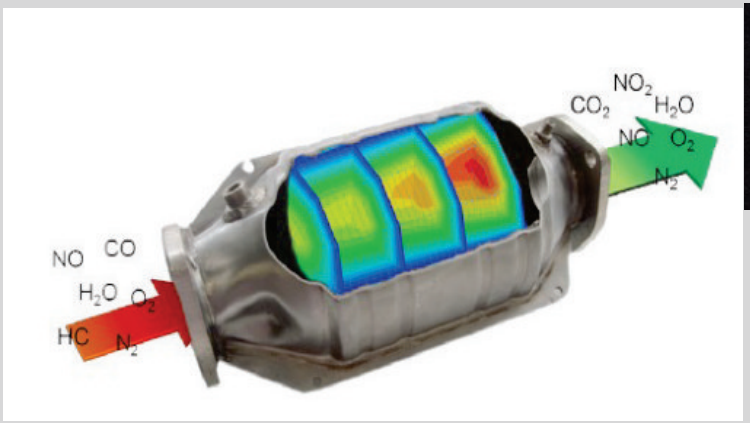
Emissionsreduzierung lokaler und globaler Schadstoffe: Forschungsresultate der Gruppe in 2018

IKFT-Seminar, 28.01.2019

Prof. Dr. Olaf Deutschmann

Institut für Technische Chemie und Polymerchemie (ITCP) Institut für Katalyseforschung und –technologie (IKFT) Abgaszentrum Karlsruhe





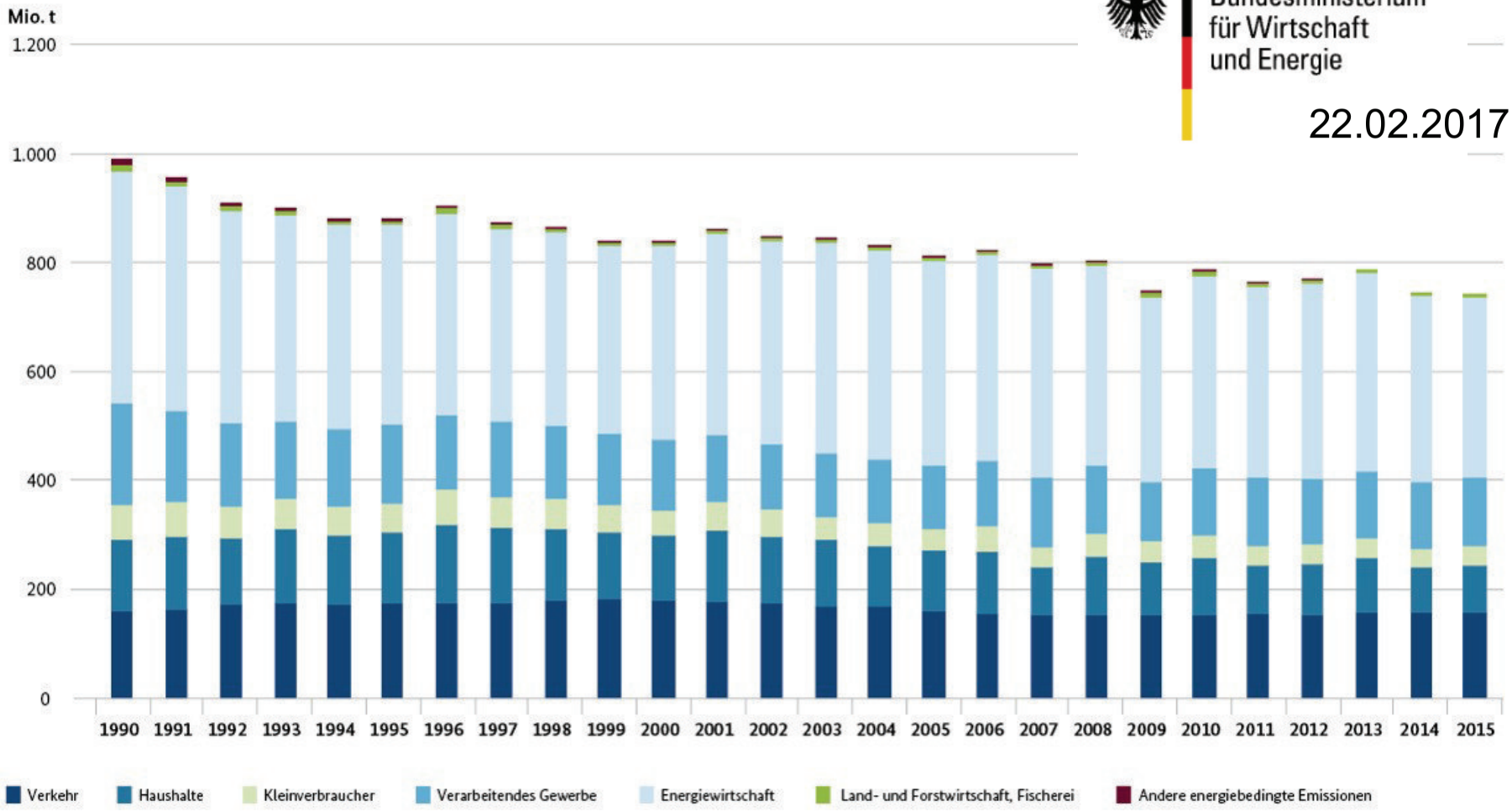


Status
Energy-caused CO_2 emissions in Germany

Karlsruhe Institute of Technology

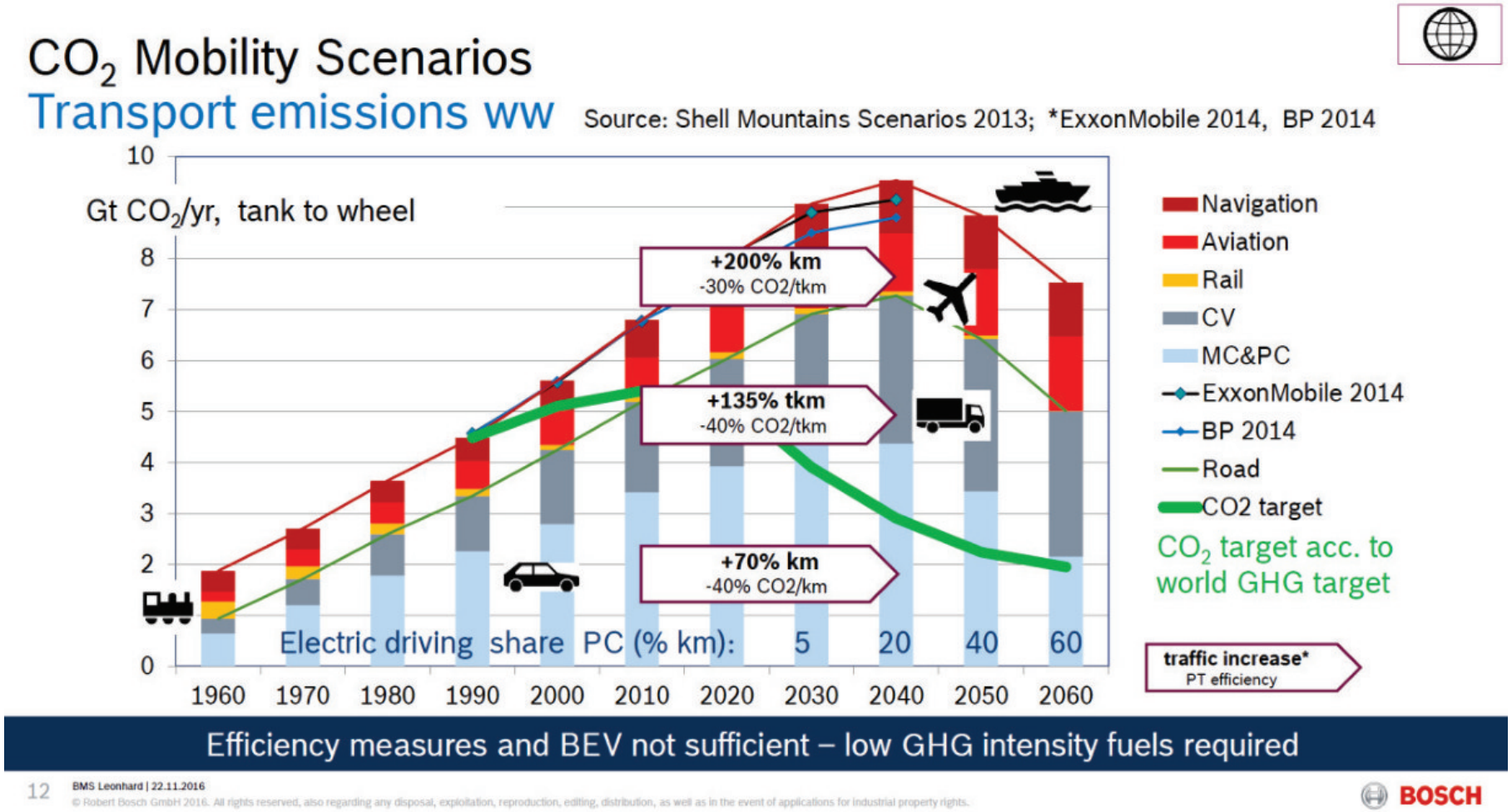
Bundesministerium für Wirtschaft und Energie

22.02.2017



Role of combustion engines

Taken from Dr. Leonhard, Bosch



Efficiency measures and BEV not sufficient – low GHG intensity fuels required

© Robert Bosch GmbH 2016. All rights reserved, also regarding any disposal, exploitation, reproduction, editing, distribution, as well as in the event of applications for industrial property rights.

Consequences of today's energy consumption: Local and global pollution of the atmosphere

Approximately 90% of the energy needed worldwide is provided by combustion processes



Combustion leads to

local

(NO_x, PM, CO, HCs, SO_x, ozone)

and

global pollution

(CO_2, CH_4, N_2O)

of the atmosphere.

Consequences of today's energy consumption: Local and global pollution of the atmosphere

Approximately 90% of the energy needed worldwide is provided by combustion processes



Combustion leads to

local

(NO_x, PM, CO, HCs, SO_x, **HCHO**…)

and

global pollution

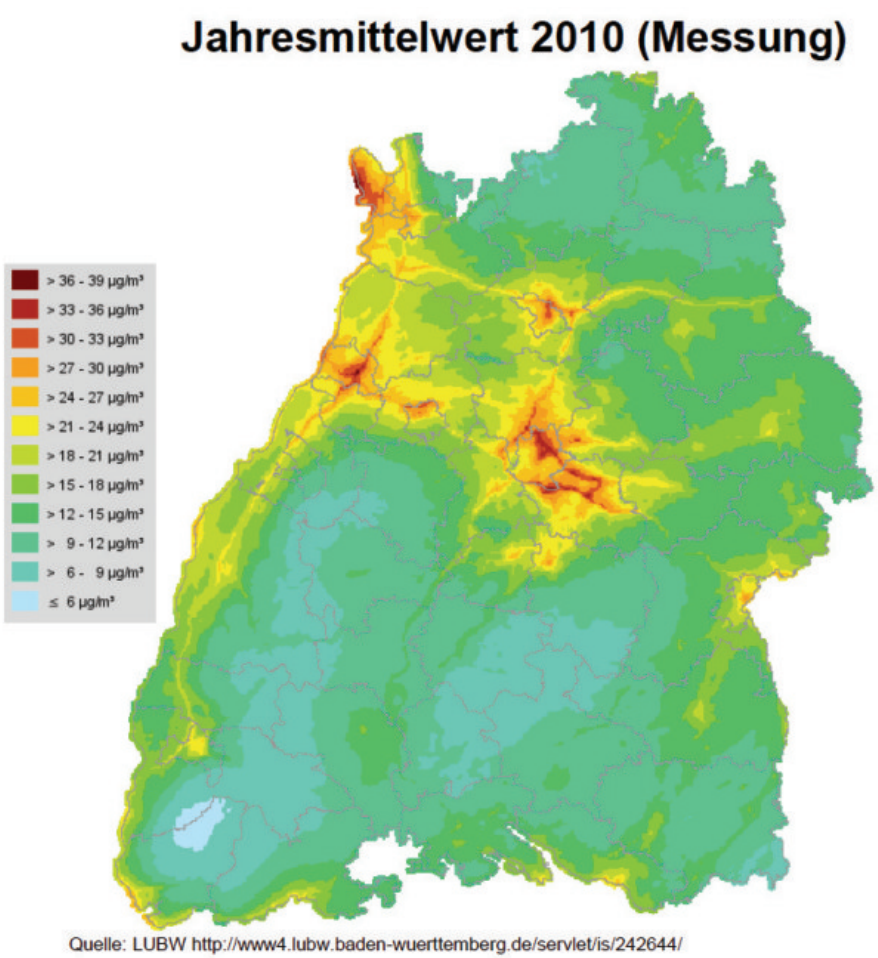
(CO_2, CH_4, N_2O…)

of the atmosphere.

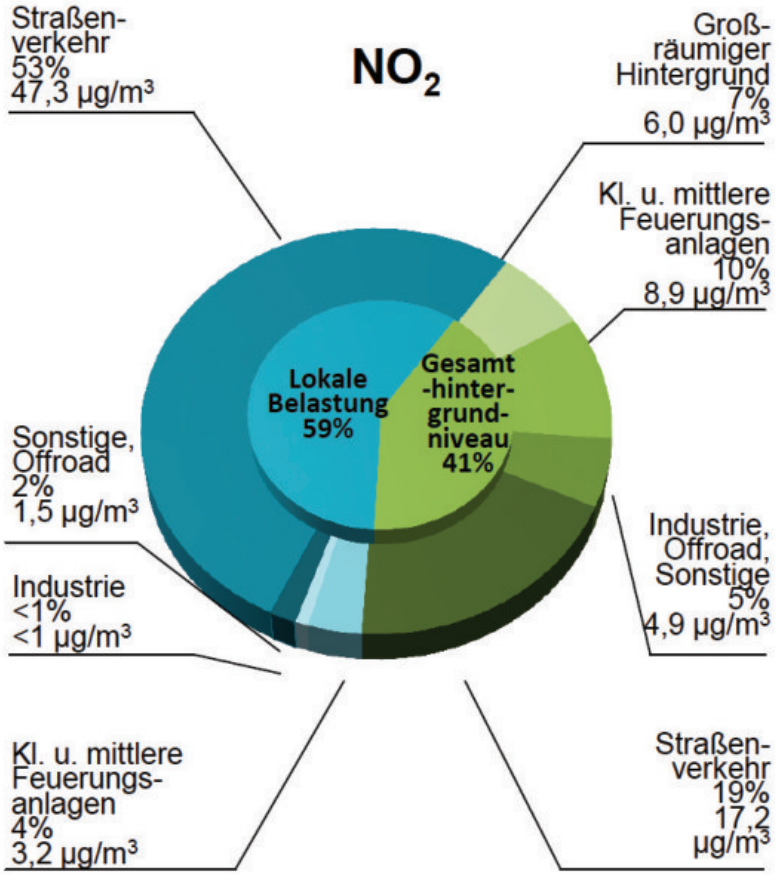
Emissionsreduzierung lokaler und globaler Schadstoffe: Forschungsresultate der Gruppe in 2018: Inhalt

- **Stickoxidemissionen aus Diesel- und Gasmotoren**
- Formaldehydemssionen aus Gasmotoren
- Methanemissionen
- CO_2-Emissionen
- Weitere Highlights

Immissionen an NO_2
Dieselfahrzeuge zweifelsfrei maßgeblicher Verursacher



Quelle: LUBW http://www4.lubw.baden-wuerttemberg.de/servlet/is/242644/



Quelle: Christoph Erdmenger; Ministerium für Transport und Infrastruktur Baden Württemberg;, IFKM/KIT – NO_X Conference, Heidelberg, 01.2016

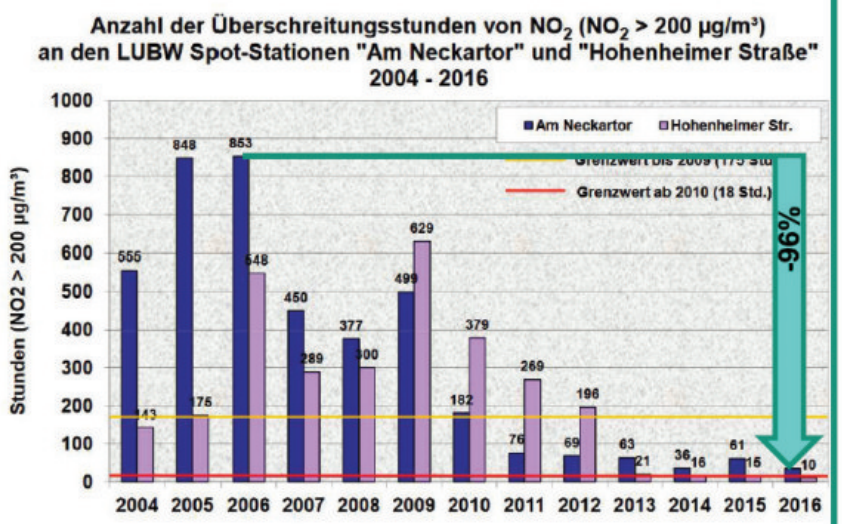
Courtesy of Prof. T. Koch, IFKM, KIT

Zeitliche Entwicklung der Immissionen an NO_2 am Hot Spots Stuttgart-Neckartor

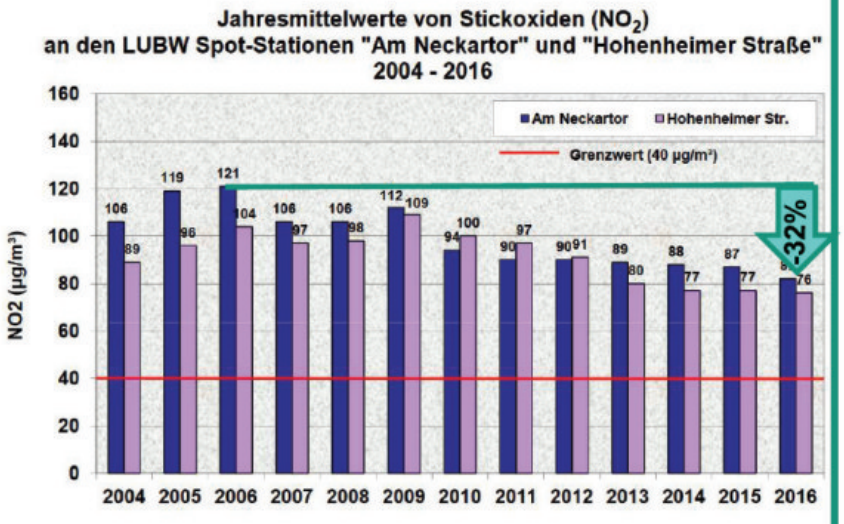


Tägliches Verkehrsvolumen in Stuttgart am Neckartor in 2012
65.980 PKW
2.200 lNfz
2.000 sNfz

Überschreitungsstunden



Jahresmittelwerte



Courtesy of Prof. T. Koch, IFKM, KIT

Wide variety of pollutants emitted from combustion engines









Gasoline *stoichiometric* *lean*

Diesel *lean*

Natural gas *stoichiometric - lean*

HC CO NO_x PM CH_4 CH_2O

Three-way catalyst

NOx storage

SCR-catalyst

PM filter

Oxidation

Ammonia slip

Hydrolysis

Pt, Pd, Rh, Ce

Pt, Pd, Rh, BaO

VO, zeolites

Pt, Pd

Selective catalytic reduction (SCR) of NO_x by urea solution: Principle

32.4% Urea-water solution (AdBlue)

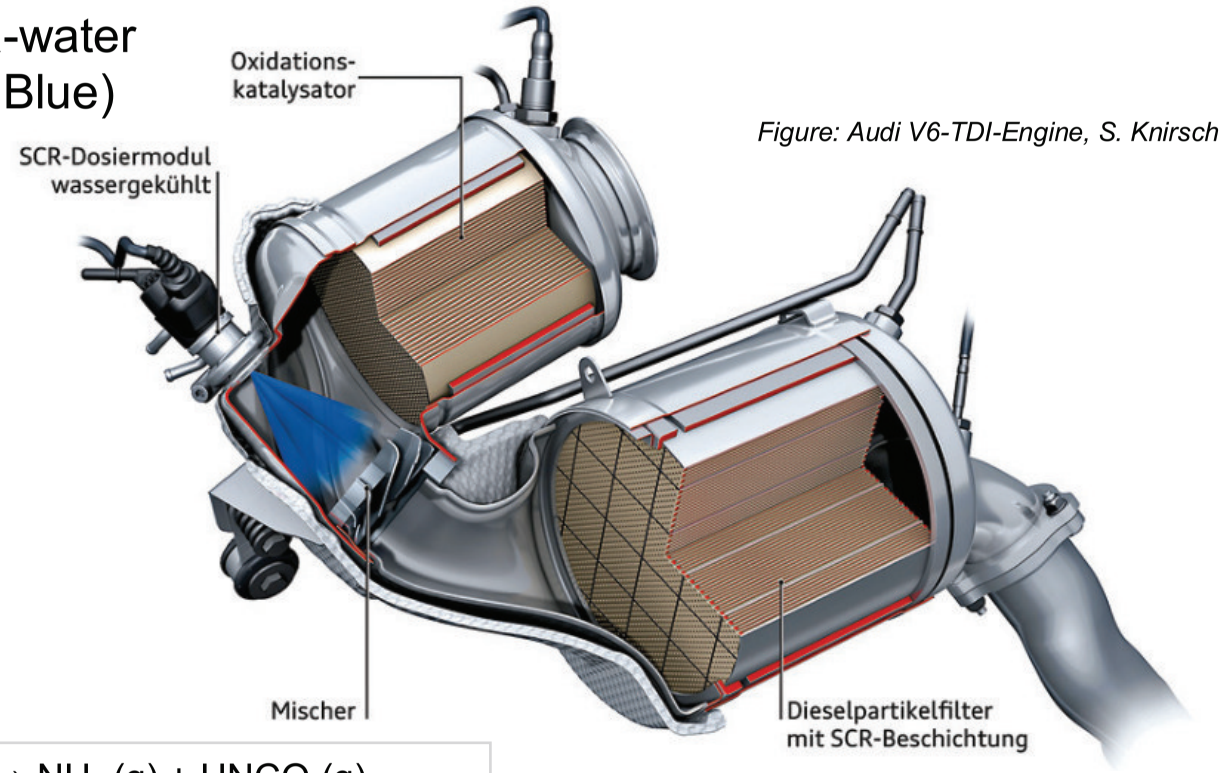


Figure: Audi V6-TDI-Engine, S. Knirsch et al., 2018

$(NH_2)_2CO\ (l) \Rightarrow NH_3\ (g) + HNCO\ (g)$

$HNCO\ (g) + H_2O\ (g) \Rightarrow NH_3\ (g) + CO_2\ (g)$

$2\ NH_3 + NO + NO_2 \rightarrow 2\ N_2 + 3\ H_2O$

Objective:
Understanding NH_3 formation from urea-water solution

32.4% Urea-water solution (AdBlue)

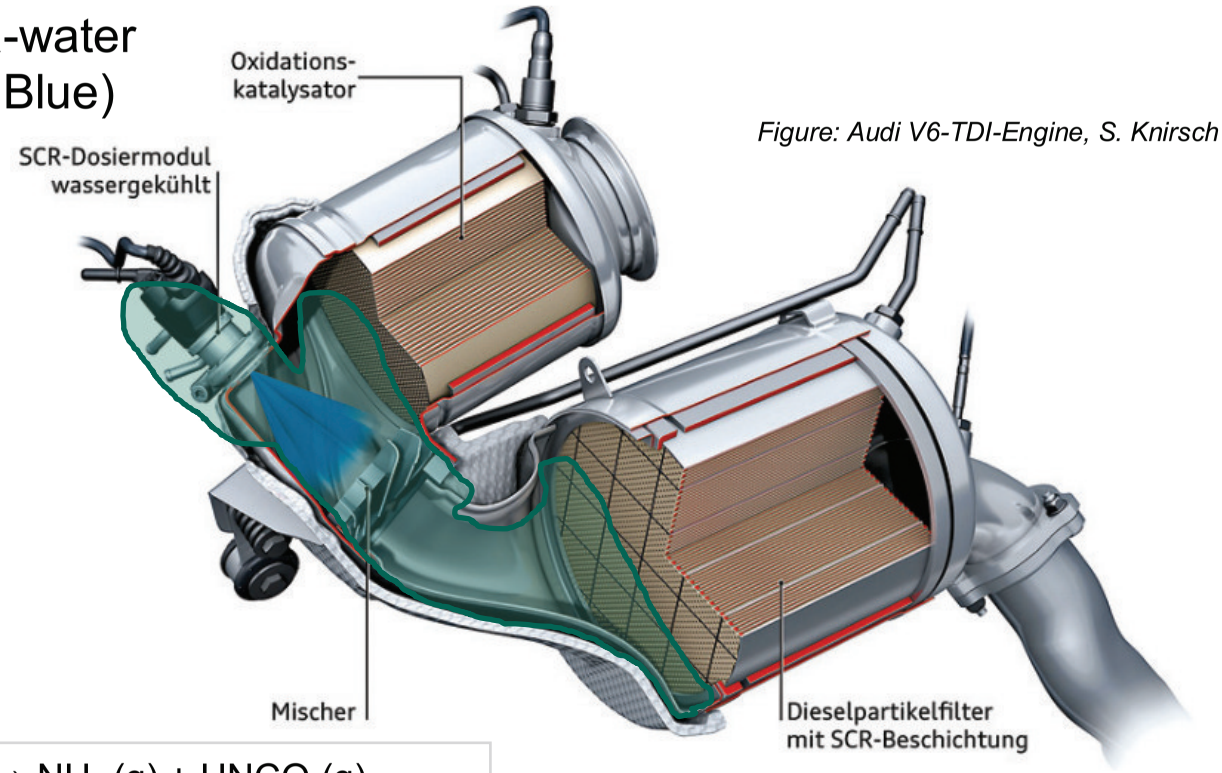


Figure: Audi V6-TDI-Engine, S. Knirsch et al., 2018

$(NH_2)_2CO\ (l) \Rightarrow NH_3\ (g) + HNCO\ (g)$

$HNCO\ (g) + H_2O\ (g) \Rightarrow NH_3\ (g) + CO_2\ (g)$

$2\ NH_3 + NO + NO_2 \rightarrow 2\ N_2 + 3\ H_2O$

Challenges in producing the reducing agent NH_3
Droplet – wall interaction

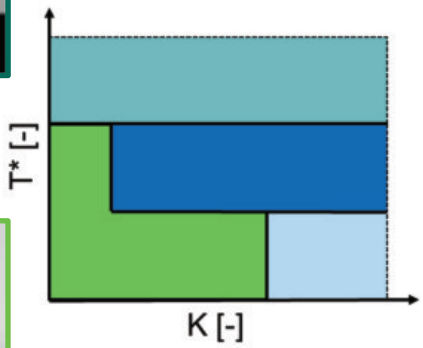
$(NH_2)_2CO$ (aq)



Droplet – wall interaction: Impact on film formation depends on temperatures and kinetic energy, and dropplet size



- Kinetic disintegration
- Secondary droplets





- Disintegration by boiling



- Oscillating spreading length and height
- No secondary droplets

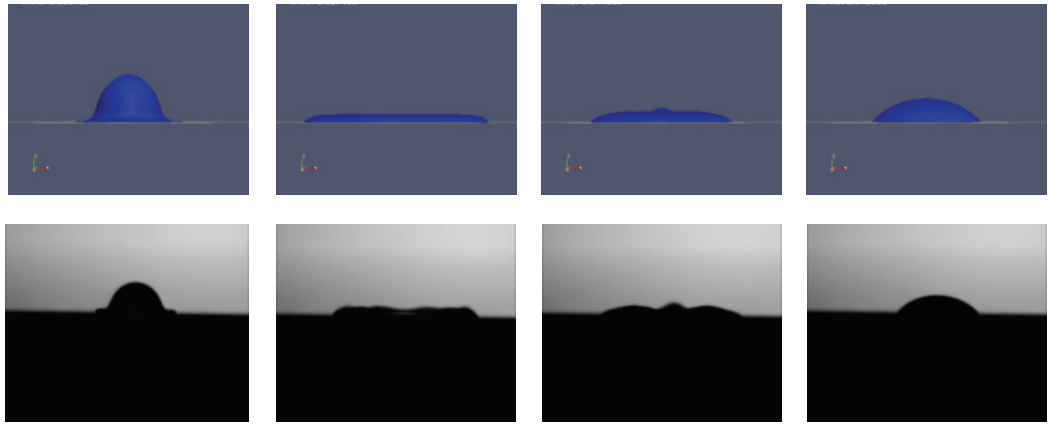


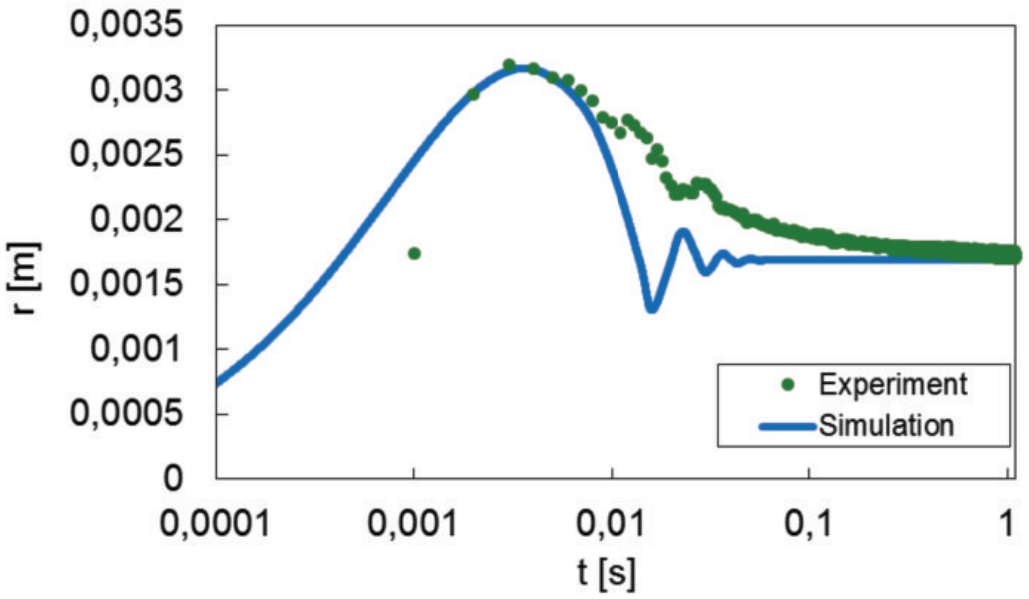
- Large spreading range
- Secondary droplets

M. Börnhorst, O. Deutschmann. International Journal of Heat and Fluid Flow 69 (2018) 55

Droplet – wall interaction
CFD simulation vs. experiment

- AdBlue droplet on stainless steel surface:
  - Diameter = 1.95 mm
  - Velocity = 1.94 m/s
  - Contact angle = 50.3°
- Simulation by OpenFoam with newely developed PhaseField method
- Disagreement in receding stage due to neglection of surface roughness in CFD

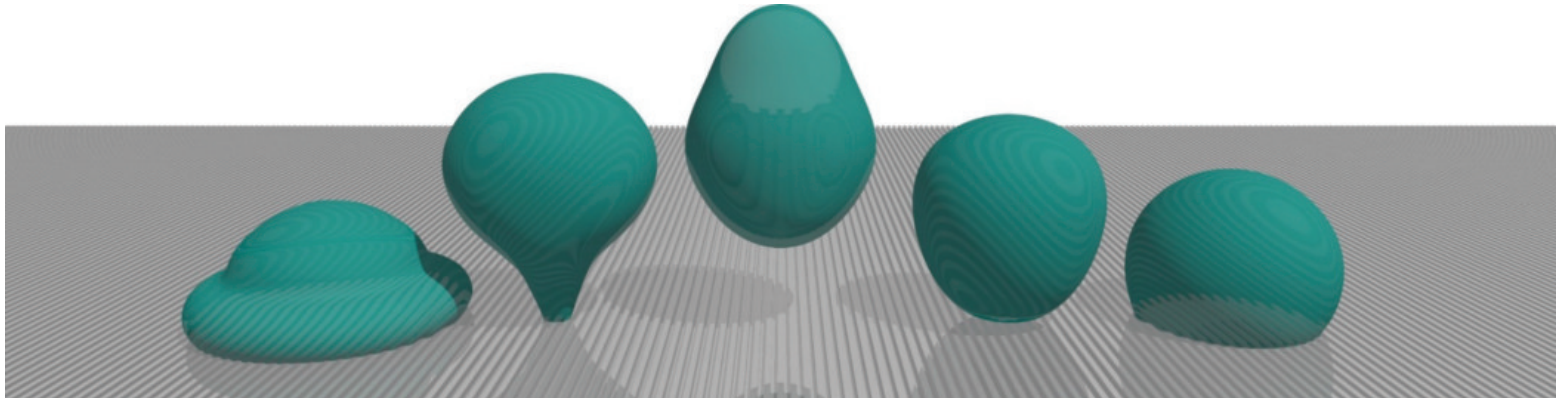




M. Börnhorst, X. Cai, M. Wörner, O. Deutschmann. Chemical Engineering & Technology, submitted

Droplet – wall interaction
CFD simulation vs. experiment

- Water droplet on hydrophobic PDMS surface
  - Diameter = 2.1 mm
  - Velocity = 0.62 m/s
  - Contact angle = 100.3°
- Phase field simulations reproduce experimental observations at ISTM
  - Drop deposits on smooth surface
  - **Drop bounces from surface structured with micro-grooves (60µm)**

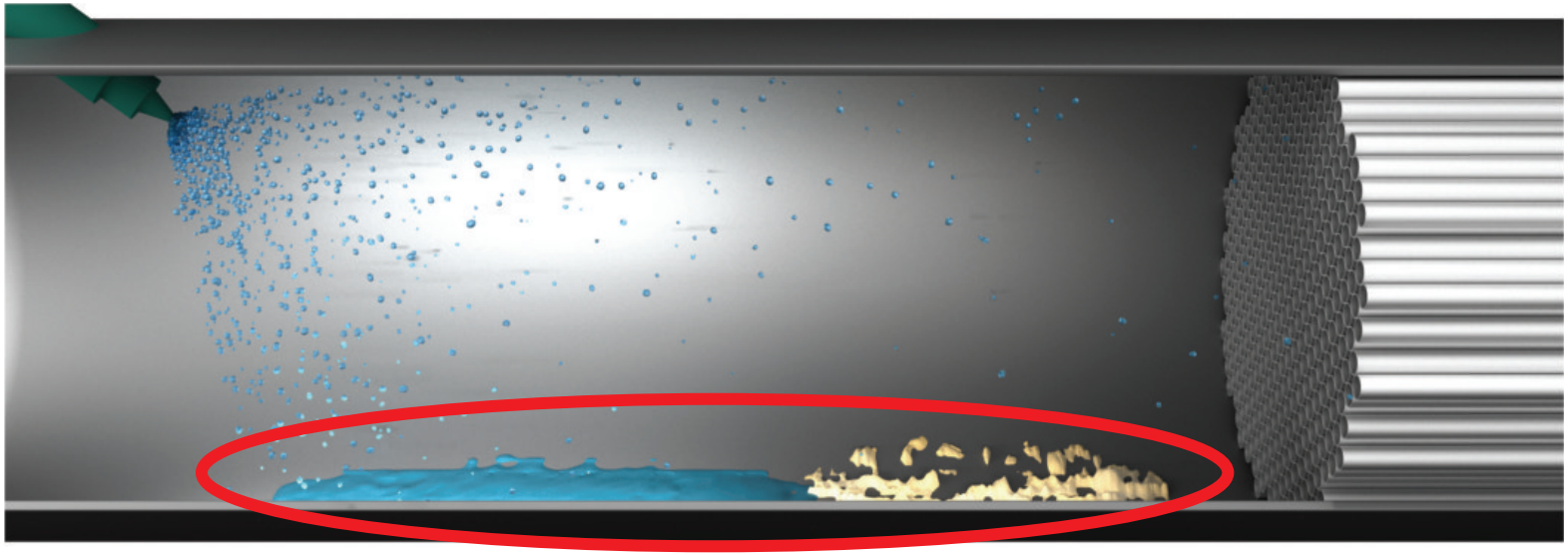


V. Fink, X. Cai, A. Stroh, R. Bernard, J. Kriegseis, B. Frohnapfel, H. Marschall, M. Wörner, Int. J. Heat Fluid Flow 70 (2018) 271-278

- Phase field method is particularly suited for wetting and microfluidics

F. Jamshidi, H. Heimel, M. Hasert, X. Cai, O. Deutschmann, H. Marschall, M. Wörner, Comput. Phys. Commun., in press
M. Wörner, X. Cai, H. Alla, P. Yue, Fluid Dyn. Res. 50 (2018) 035501

Challenges in producing the reducing agent NH_3
Formation of liquid films and solid deposits



Urea solution dosage:
Interaction of existing deposits with spray



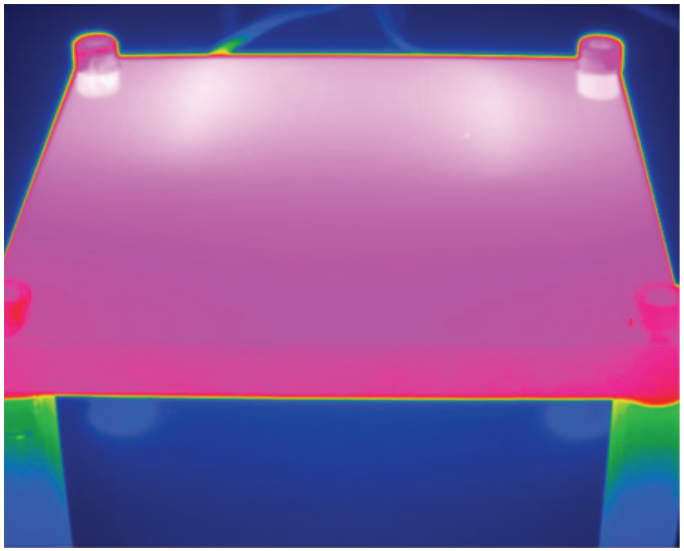
- Multiple injections at T_{gas} = 300°C
- Dissolution of existing deposits in injected solution
- Re-start of decomposition process
- Solid deposits formed



Top view into the injection chamber of experimental test rig

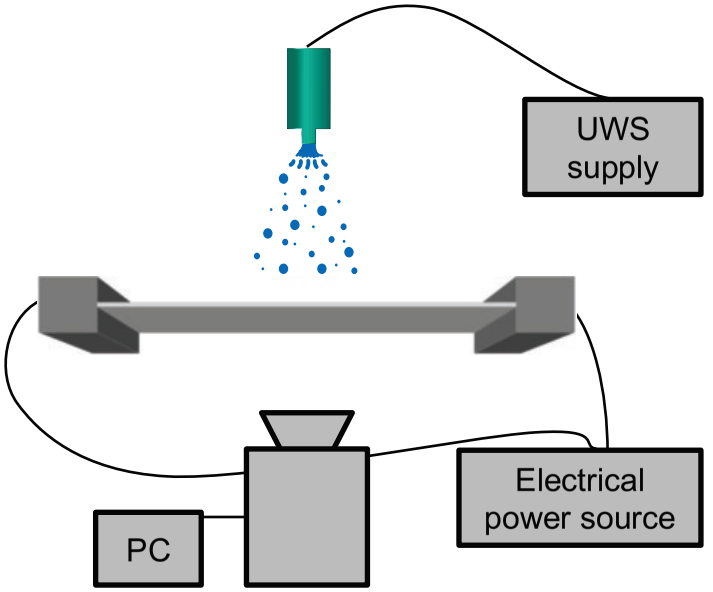
M. Börnhorst, S. Langheck, H. Weickenmeier, C. Dem, R. Suntz, O. Deutschmann. Chemical Engineering Journal, doi.org/10.1016/j.cej.2018.09.016

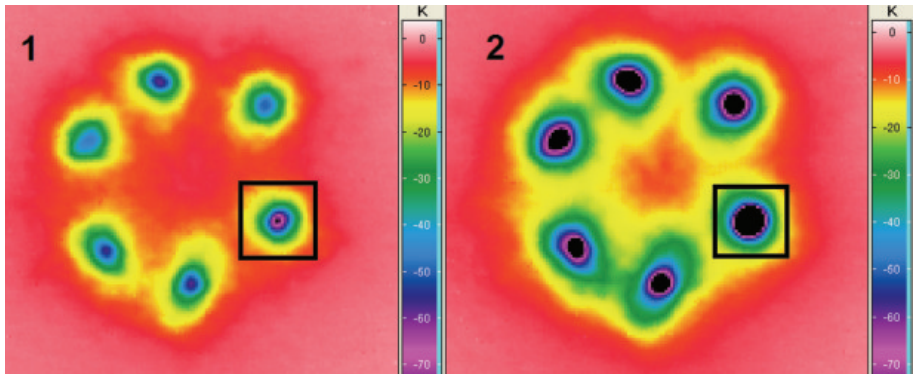
Urea solution dosage: Cooling of film and wall



T_w = 280°C

TV = 10 %
t_{akt} = 3 s





- Thermographic imaging of spray impact at 60 Hz
- Substrate: 0.1 mm Inconel alloy sheet
- Heating by high electrical resistance

M. Börnhorst, S. Langheck, H. Weickenmeier, C. Dem, R. Suntz, O. Deutschmann. Chemical Engineering Journal, doi.org/10.1016/j.cej.2018.09.016

Challenges in producing the reducing agent NH_3
Formation of solid urea by-products

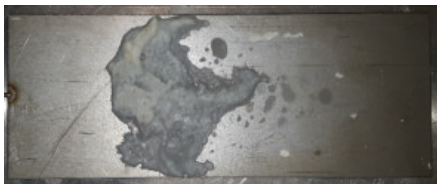
- Samples of solid deposits taking from the tailpipe of a commercial large diesel engine operated with urea-SCR



Size: 10 cm

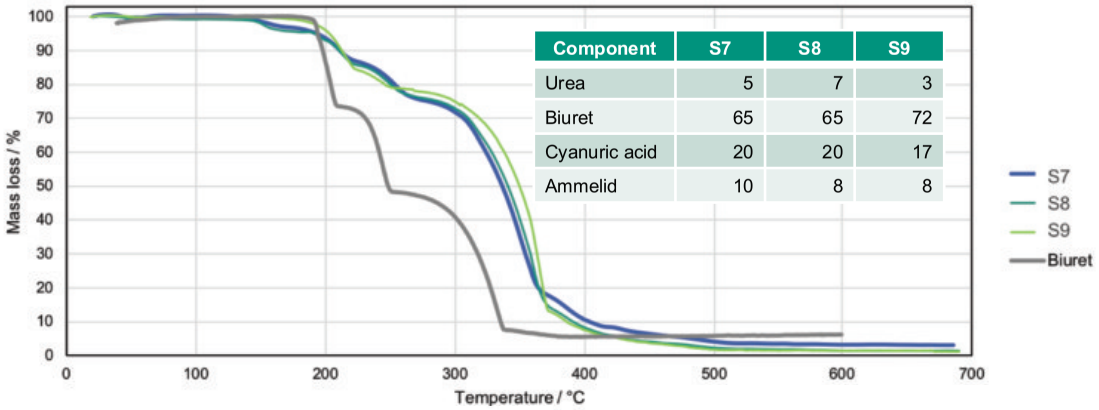
Analysis of deposits formed from urea by TGA and HPLC: Variation of chemical composition and topology

Samples are taken from large diesel engines´ tailpipe

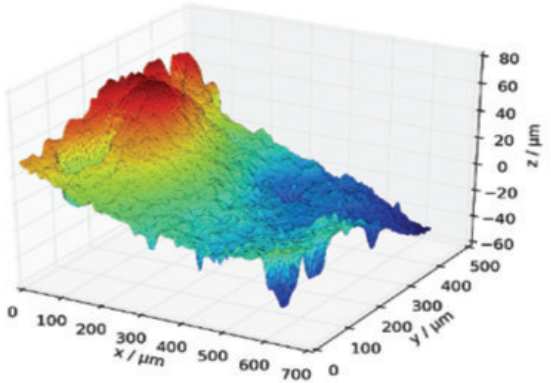




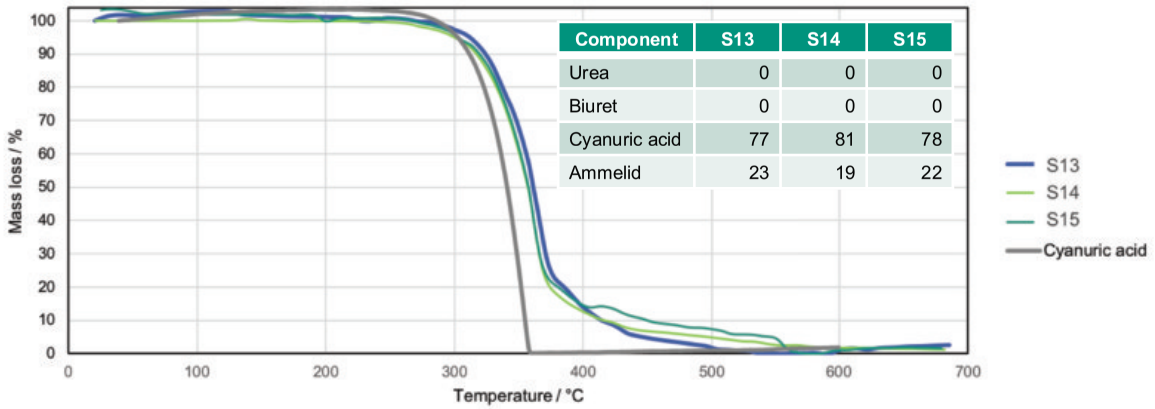
Rig 1, T = 300°C
Urea conc. 32.5 %



Component	S7	S8	S9
Urea	5	7	3
Biuret	65	65	72
Cyanuric acid	20	20	17
Ammelid	10	8	8



Rig 2, T = 320°C
Urea conc. 32,5 %



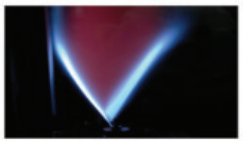
Component	S13	S14	S15
Urea	0	0	0
Biuret	0	0	0
Cyanuric acid	77	81	78
Ammelid	23	19	22

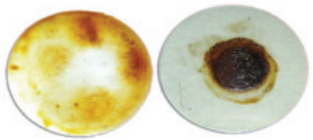
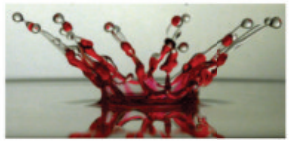
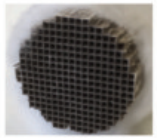
M. Börnhorst, H. Weickenmeier, M, Casapu, S. Schwartz, Sonja Habicht, 2018

SFB/TRR 150: Turbulente, chemisch reagierende Mehrphasenströmungen in Wandnähe (TU Darmstadt/KIT) Erfolgreiche Begutachtung Herbst 2018

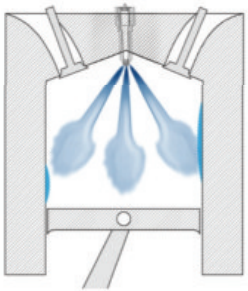
Motivation

Turbulente, chemisch reagierende Mehrphasenströmungen
werden **durch Wände stark beeinflusst**.



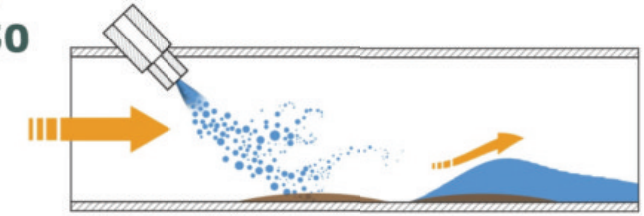




Einzelmechanismen und Zusammenwirken **unzureichend bekannt**



Innermotorische Verbrennung

Leitbeispiele des SFB/Transregio 150



Mehrphasenprozesse bei Abgasreinigung

neue Technologiekonzepte erfordern **detaillierte Kenntnisse** wandnaher Prozesse

Zusammenarbeit: Abgasstrang

Mechanismen, Sensitivitäten

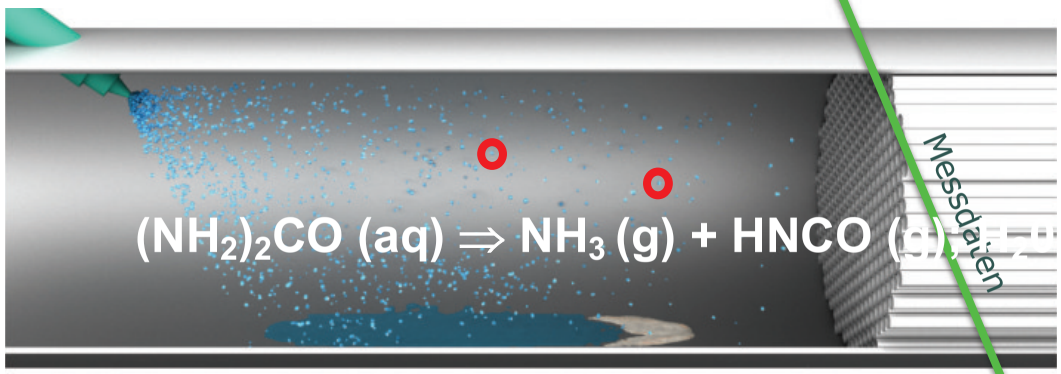
B04 **Olzmann:** Elementar-reaktionen

Submech-anismen

B05 **Deutschmann:** Modellierung und Simulation mehrphasiger chemischer Reaktionen

Mech-anismen

B07 **Bykov/Maas:** Modell-reduktion für Reaktions-Transport-Systeme




International Journal of Heat and Fluid Flow 70 (2018) 216–225

Contents lists available at ScienceDirect

International Journal of Heat and Fluid Flow

journal homepage: www.elsevier.com/locate/ijhff

A reduced model for the evaporation and decomposition of urea–water solution droplets

M. Stein[a,*], V. Bykov[a], A. Bertótiné Abai[b], C. Janzer[c], U. Maas[a], O. Deutschmann[b], M. Olzmann[c]

C04 **Deutschmann/Suntz:** Experi-mentelle Untersuchung chemischer mehrphasiger Reaktionen

SFB/Transregio 150

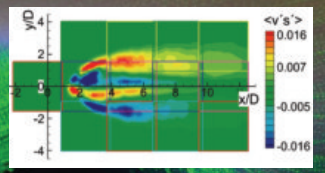
Turbulente, chemisch reagierende Mehrphasenströmungen in Wandnähe

TECHNISCHE UNIVERSITÄT DARMSTADT

KIT Karlsruher Institut für Technologie

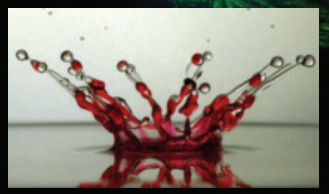
2. Förderphase für 2019-2022 bewilligt

TP A06 Experimentelle Untersuchung der Wechselwirkung zwischen Skalartransport und Turbulenz an Wänden



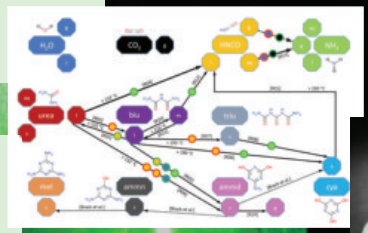


TP B08 Numerische Simulation der Tropfen-Wandfilm-Wechselwirkung von mischbaren Flüssigkeiten





TP B05 Modellierung und numerische Simulation mehrphasiger chemischer Reaktionen in Abgasnachbehandlungssystemen



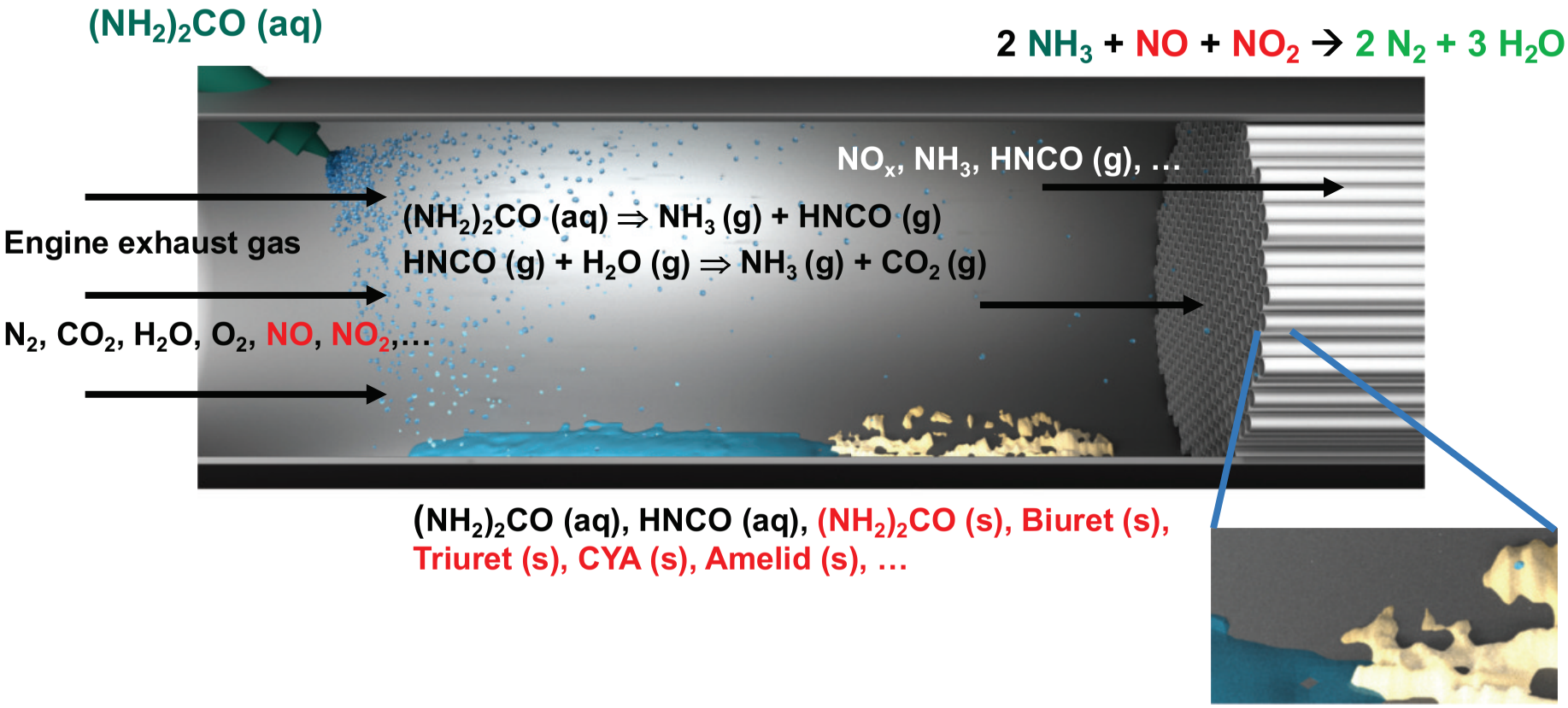


TP C04 Experimentelle Untersuchung chemischer, mehrphasiger Reaktionen in Abgasnachbehandlungssystemen

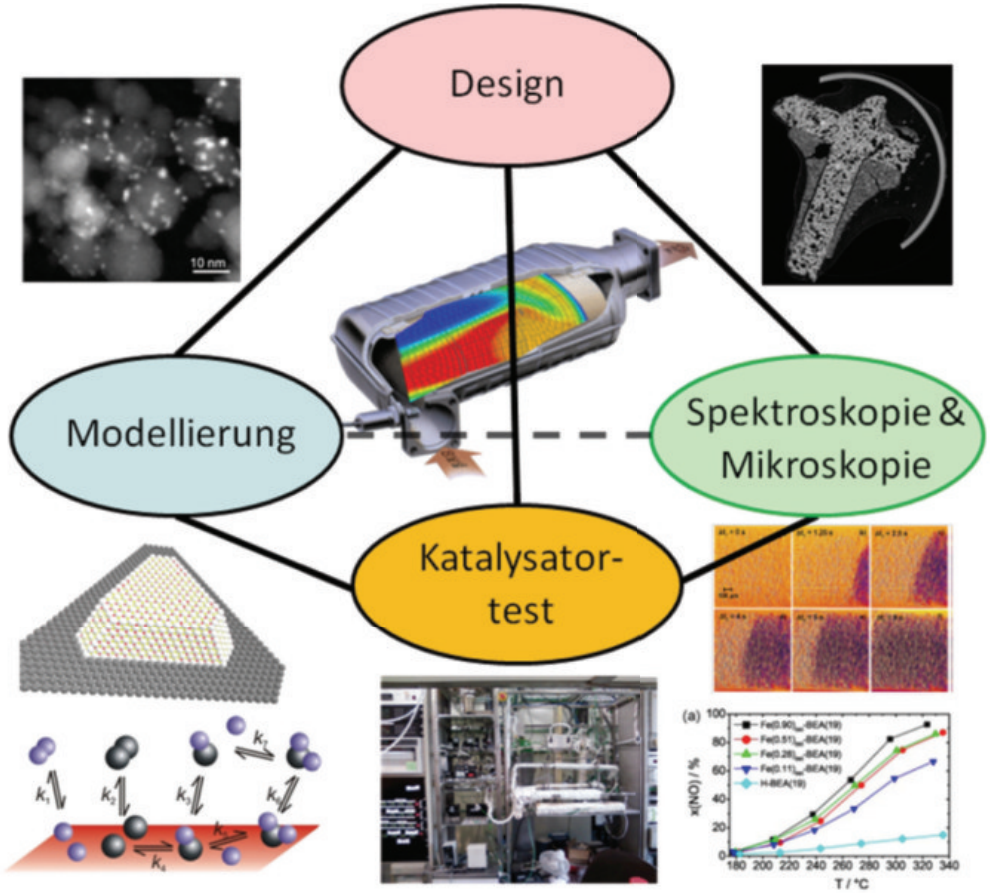




Themenschwerpunkt: Abgasstrang 2. Förderphase

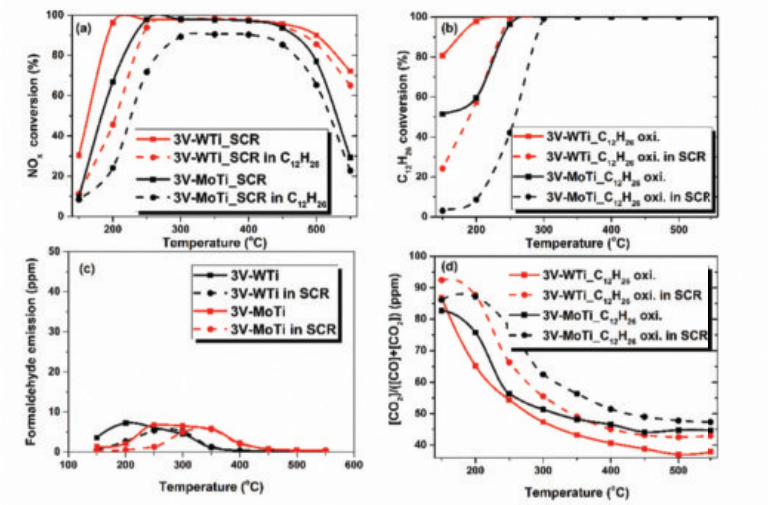


Abgaszentrum Karlsruhe: Gemeinsame Forschung der Arbeitsgruppen Grunwaldt und Deutschmann



O. Deutschmann, J.-D. Grunwaldt, Chem. Ing. Techn. 85, 595 (2013)

Standard SCR in presence of dodecane oxidation



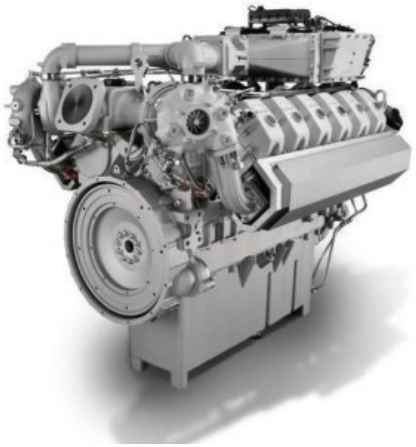
L. Zheng, M. Casapu, M. Stehle, O. Deutschmann, J.-D. Grunwaldt. Selective catalytic reduction of NOx with ammonia and hydrocarbon oxidation over V2O5-MoO3/TiO2 and V2O5-WO3/TiO2 SCR catalysts. Topics in Catalysis (2018)

Natural gas engines:
Climate-friendly concerning CO_2 but …

- About 30% reduction in CO_2 emissions at given power
- Emissions control required







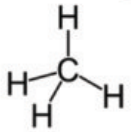
N_2
H_2O
O_2
CO_2



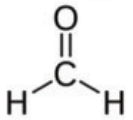
N_2
H_2O
O_2
CO_2

CO
NO_x
CH_4
NMHC
CH_2O
SO_2

green house gas



carcinogenic



SO_2

Emissionsreduzierung lokaler und globaler Schadstoffe: Forschungsresultate der Gruppe in 2018: Inhalt

- Stickoxidemissionen aus Diesel- und Gasmotoren
- **Formaldehydemssionen aus Gasmotoren**
- Methanemissionen
- CO_2-Emissionen
- Weitere Highlights

Impact of gas mixture and aging conditions on formaldehyde conversion over a series of commercial Pt-based catalysts

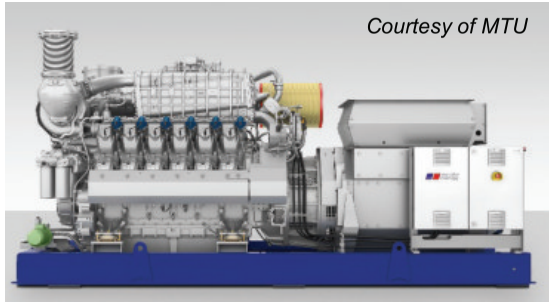


FIGURE 9 Formaldehyde conversion (3rd light off) of the 5 industrial catalysts in simulated exhaust gas after field aging for 4809 h (details, cf. text).

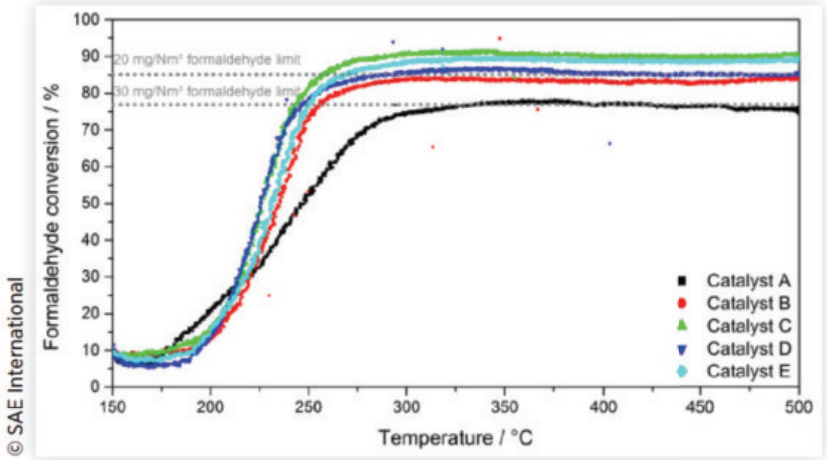
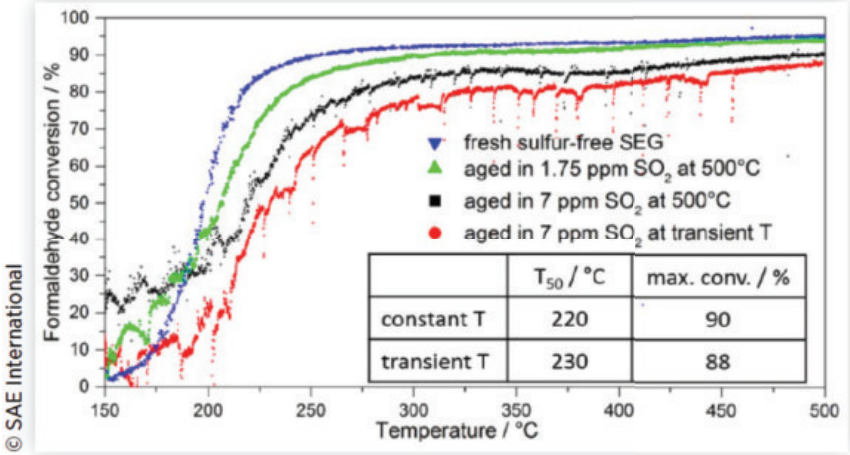


FIGURE 6 Formaldehyde conversion (3rd light off) for catalyst C: ▼ - fresh in sulfur-free SEG, ▲ - after aging for 100 h at 500 °C in the presence of 1.75 ppm SO_2 ■ - after aging for 100 h at 500 °C in the presence of 7 ppm SO_2, ●: after transient ageing by cycling between 150 and 500 °C. Gas mixture: 80 ppm HCHO, 1500 ppm CH_4, 700 ppm CO, 100 ppm C_2H_6, 50 ppm C_2H_4, 20 ppm C_3H_6, 250 ppm NO, 100 ppm NO_2, 12 Vol.-% H_2O, 10 Vol.-% O_2, 6 Vol.-% CO_2, GHSV = 100,000 h^{-1}.

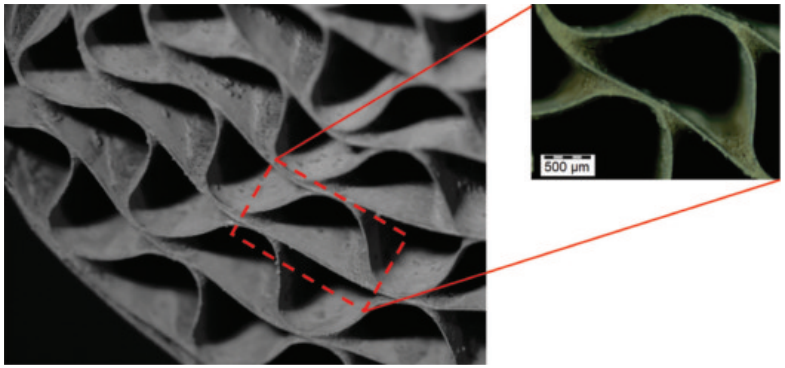


	T_{50} / °C	max. conv. / %
constant T	220	90
transient T	230	88

T. Schedlbauer, A. Gremminger, M. Casapu, O. Deutschmann, J.-D. Grunwaldt. SAE Technical Paper 2018-01-5021 (2018)

Non-uniform catalyst distribution: Ultra-low emission limits affected by mass transport limitations

- Pt-based catalyst for oxidation of formaldehyde emitted from large gas engines



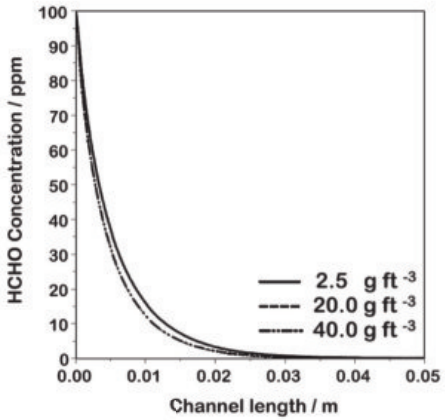
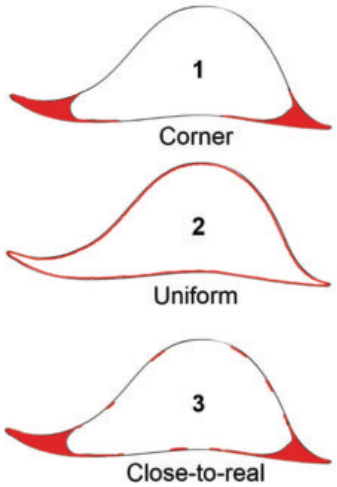
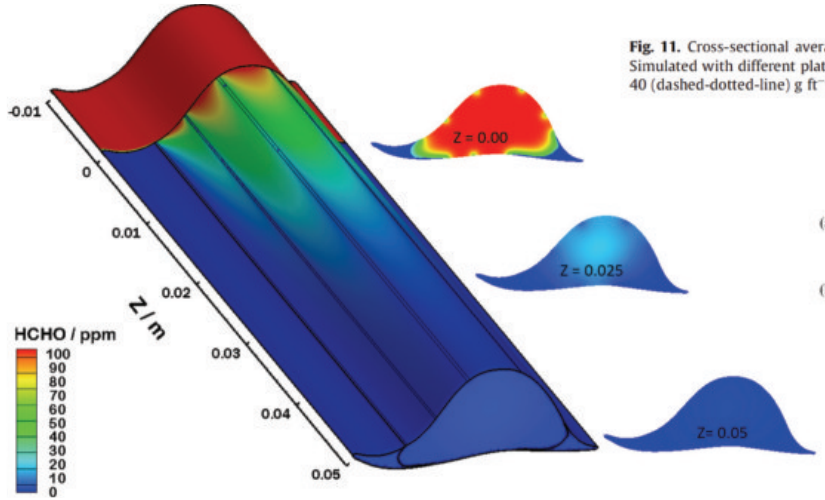
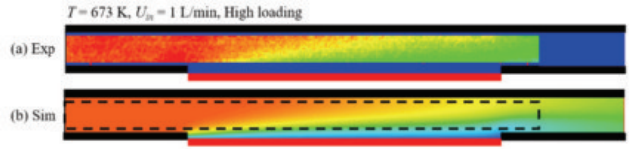


Fig. 11. Cross-sectional averaged concentration vs. channel length (second case). Simulated with different platinum loading of 2.5 (solid line), 20 (dashed-line) and 40 (dashed-dotted-line) g ft^{-3}.



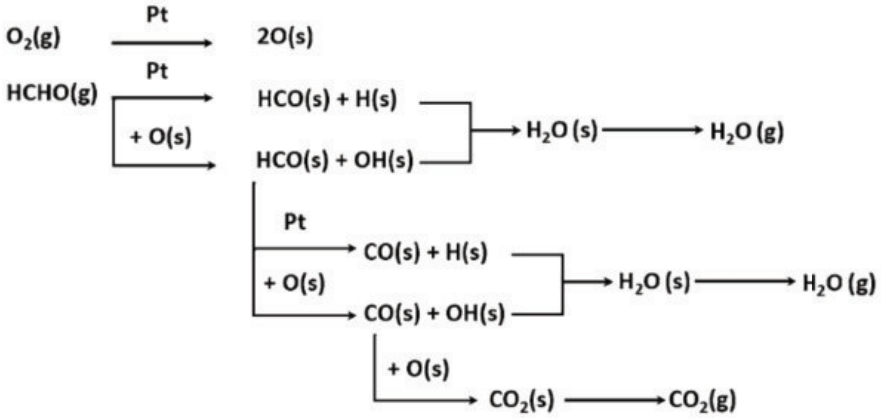


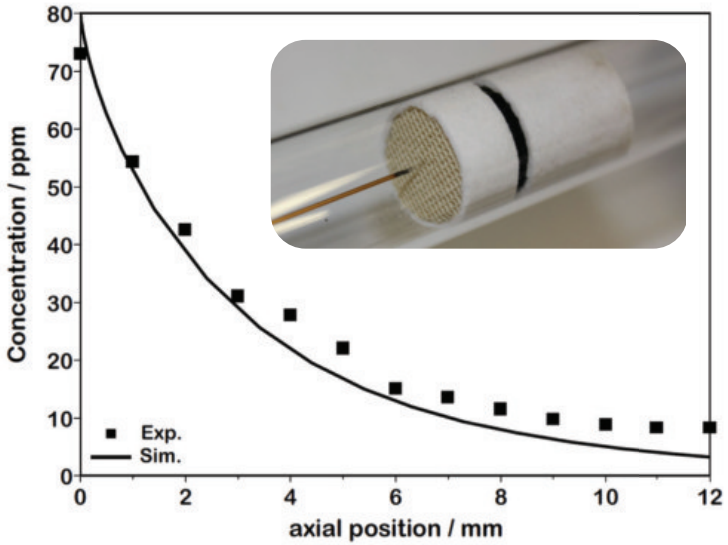


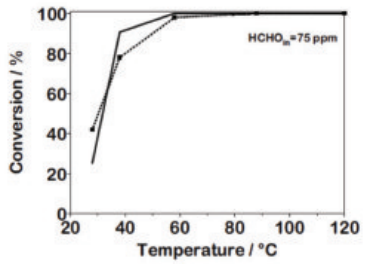
Sui Wan, T. Häber, R. Suntz, O. Deutschmann, 2019

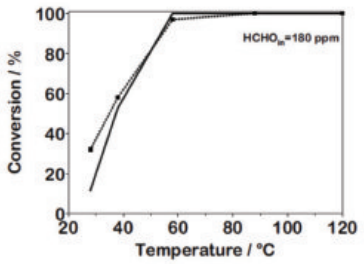
B. Torkashvand, L. Maier, M. Hettel, T. Schedlbauer, J.-D. Grunwaldt, O. Deutschmann, Chem. Eng. Sci., doi.org/10.1016/j.ces.2018.10.031

Formaldehyde Oxidation over Platinum: On the Kinetics Relevant to Exhaust Conditions of Lean-Burn Natural Gas Engines









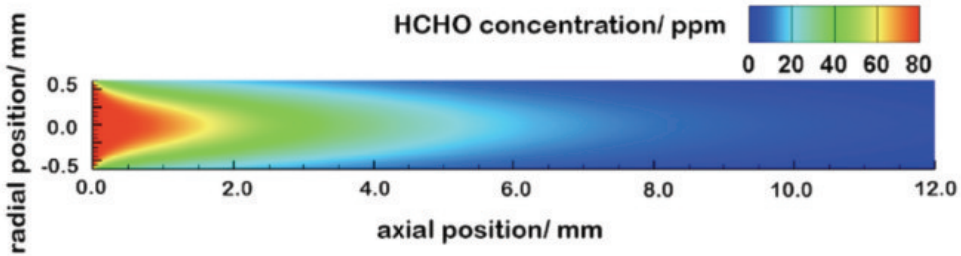


Fig. 5 Experimental (dashed lines with squares) and simulated (solid lines) conversion of formaldehyde as a function of temperature for 75 ppm (left), 180 ppm (middle) and 300 ppm (right) formaldehyde in 22 vol% O_2 balanced in N_2

B. Torkashvand, L. Maier; P. Lott, T. Schedlbauer, J.-D. Grunwaldt, O. Deutschmann. Topics in Catalysis, doi.org/10.1007/s1124 4-018-1087-y

Support effects and SO_2 poisoning of Pt-based HCHO oxidation catalysts: Catalyst characterization leads to understanding

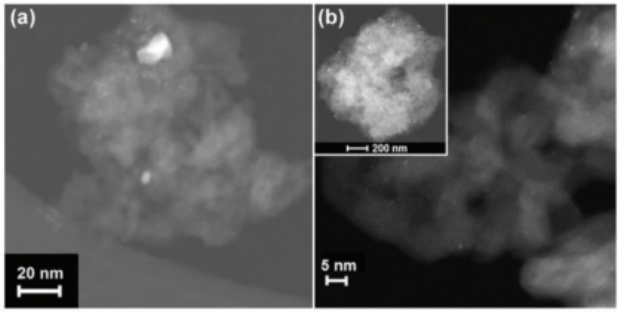


Fig. 1 HAADF STEM images of the fresh catalysts: **a** 0.5 wt% Pt/Al_2O_3 and **b** 0.5 wt% Pt/TiO_2–SiO_2

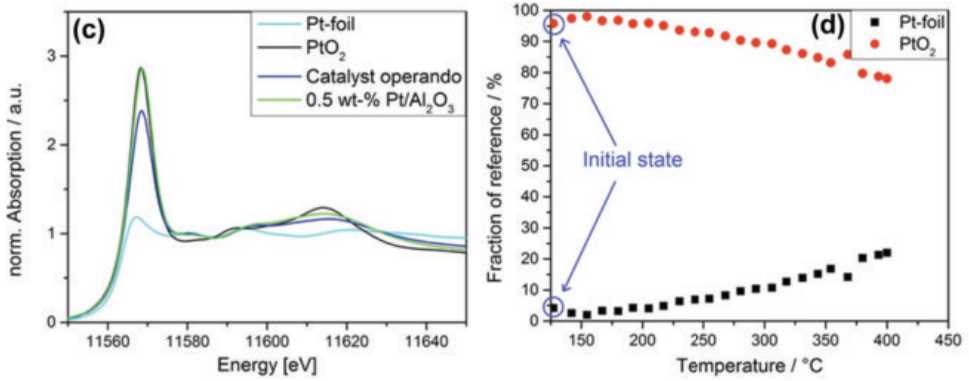
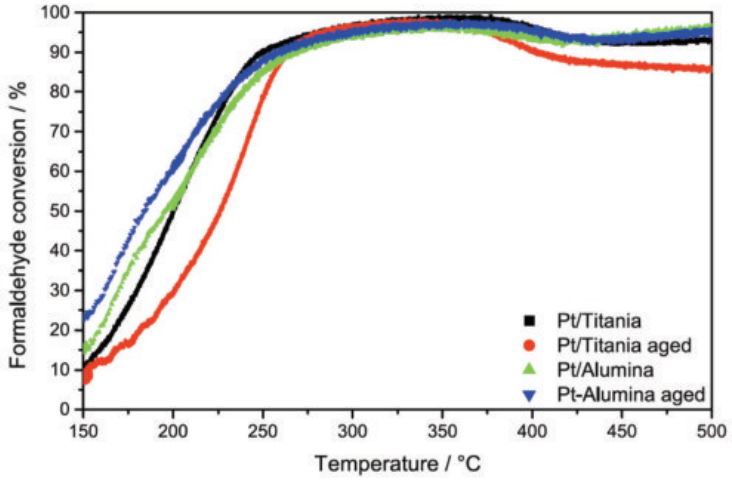
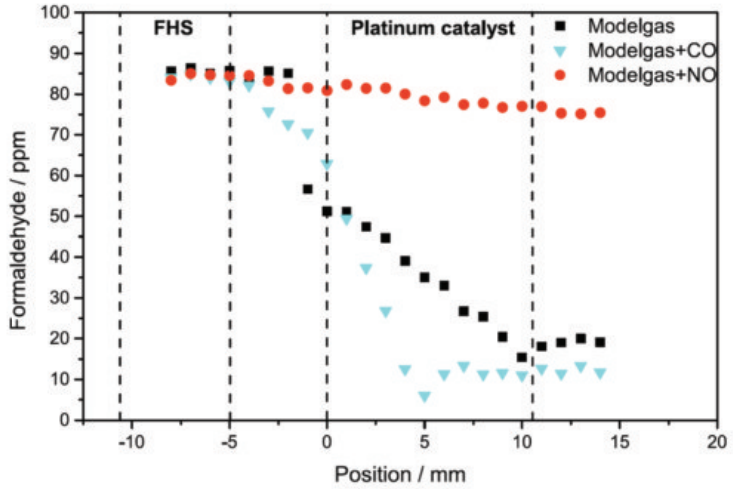


Fig. 2 Normalized XANES spectra collected at room temperature for the as prepared catalysts (green), catalysts after formaldehyde oxidation in 80 ppm HCHO, 10% O_2/He (dark blue) and PtO_2 and Pt-foil as references: **a** 0.5 wt% Pt/TiO_2–SiO_2 and **c** 0.5 wt% Pt/Al_2O_3 **b** LCF analysis of operando XANES of 0.5 wt% Pt/TiO_2–SiO_2. **d** LCF analysis of operando XANES of 0.5 wt% Pt/Al_2O_3



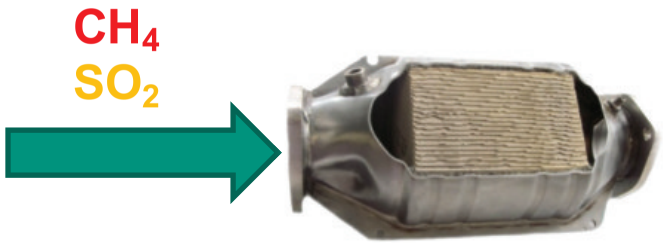


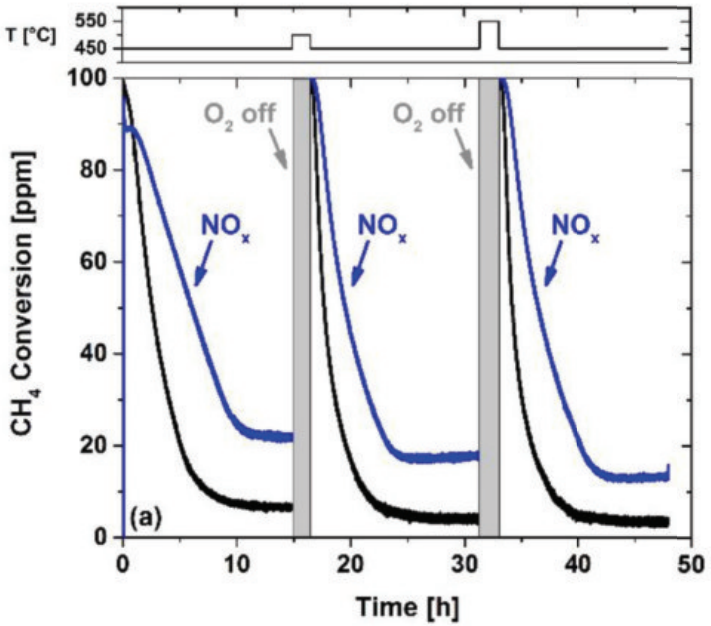
T. Schedlbauer, P. Lott, M. Casapu, H. Störmer, O. Deutschmann, J.-D. Grunwaldt. Topics in Catalysis, doi.org/10.1007/s11244-018-1122-z

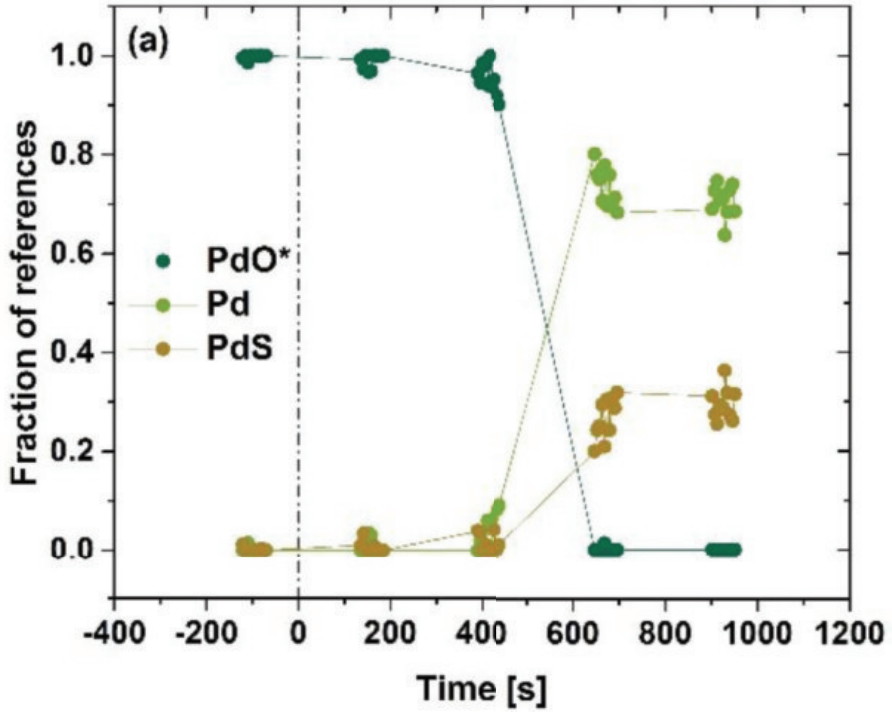
Emissionsreduzierung lokaler und globaler Schadstoffe: Forschungsresultate der Gruppe in 2018: Inhalt

- Stickoxidemissionen aus Diesel- und Gasmotoren
- Formaldehydemssionen aus Gasmotoren
- **Methanemissionen**
- CO_2-Emissionen
- Weitere Highlights

Regeneration of sulfur poisoned Pd-Pt/CeO_2-ZrO_2-Y_2O_3-La_2O_3 and Pd-Pt/Al_2O_3 methane oxidation catalysts





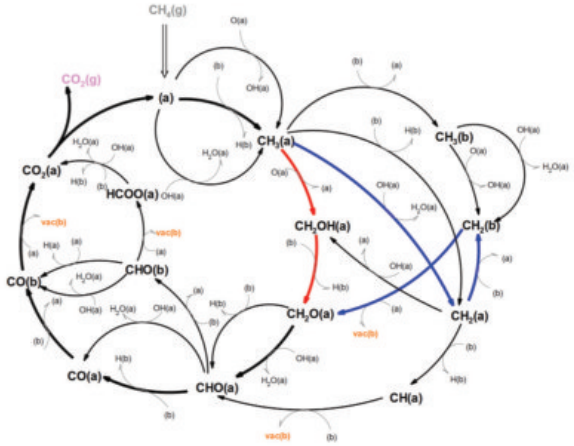


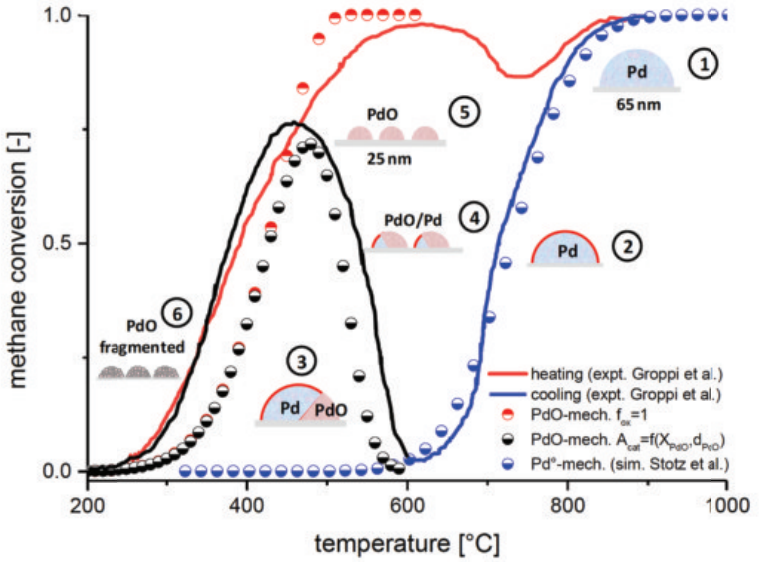
P. Lott, M. Eck, D.E. Doronkin, R. Popescu, M. Casapu, J.-D. Grunwaldt, O. Deutschmann. Topics in Catalysis, doi.org/10.1007/s11244-018-1121-0

Surface Reaction Kinetics of Methane Oxidation over PdO: Development of a detailed reaction mechanism

Karlsruhe Institute of Technology

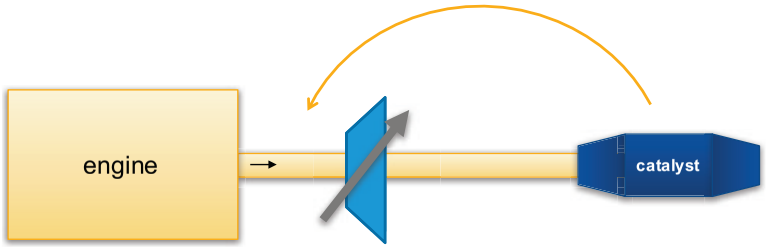
No.	Adsorption/Desorption Reaction	forward reaction s^0 [-]	β_f [-]	$E_{a,f}$ [kJ/mol]	reverse reaction A_r [mol,cm,s]	β_r [-]	$E_{a,r}$ [kJ/mol]
R1	$CH_4(g) + (a) + (b) \rightleftharpoons CH_3(a) + H(b)$	$4.582 \cdot 10^{-02}$	-0.001	33.155	$1.034 \cdot 10^{+21}$	0.003	106.180
R2	$CH_4(g) + OH(a) + (a) \rightleftharpoons CH_3(a) + H_2O(a)$	$1.510 \cdot 10^{-02}$	0.001	28.86	$7.071 \cdot 10^{+19}$	-0.004	104.259
R3	$CH_4(g) + O(a) + (a) \rightleftharpoons CH_3(a) + OH(a)$	$3.082 \cdot 10^{-02}$	0.007	26.234	$2.695 \cdot 10^{+20}$	-0.029	192.865
R4	$O_2(g) + (a) \rightleftharpoons O_2(a)$	$5.710 \cdot 10^{-02}$	0.0	0.0	$6.702 \cdot 10^{+15}$	-0.031	63.541
R5	$O_2(g) + vac(b) \rightleftharpoons O(b)$	$5.710 \cdot 10^{-02}$	0.0	0.0	$7.024 \cdot 10^{+15}$	-0.027	159.975
R6	$H_2O(g) + O(a) + (a) \rightleftharpoons 2\ OH(a)$	$1.400 \cdot 10^{-01}$	0.0	0.0	$3.307 \cdot 10^{+20}$	0.013	191.178
R7	$H_2O(g) + (a) \rightleftharpoons H_2O(a)$	$1.400 \cdot 10^{-01}$	0.0	0.0	$6.293 \cdot 10^{+12}$	0.045	99.946
R8	$CO_2(g) + (a) \rightleftharpoons CO_2(a)$	$4.910 \cdot 10^{-02}$	0.0	0.0	$4.087 \cdot 10^{+14}$	0.029	65.097
No.	Surface Reactions	A_f [mol,cm,s]	β_f [-]	$E_{a,f}$ [kJ/mol]	A_r [mol,cm,s]	β_r [-]	$E_{a,r}$ [kJ/mol]
R9	$CH_3(a) + (b) \rightleftharpoons CH_3(b) + (a)$	$1.494 \cdot 10^{+22}$	0.008	131.139	$2.441 \cdot 10^{+23}$	0.008	181.201
R10	$CH_3(b) + O(a) \rightleftharpoons CH_2(b) + OH(a)$	$1.250 \cdot 10^{+22}$	0.012	33.366	$1.855 \cdot 10^{+22}$	-0.012	303.074
R11	$CH_3(b) + OH(a) \rightleftharpoons CH_2(b) + H_2O(a)$	$1.398 \cdot 10^{+22}$	-0.004	33.193	$1.111 \cdot 10^{+22}$	0.004	221.667
R12	$CH_3(a) + O(a) \rightleftharpoons CH_2OH(a) + (a)$	$3.534 \cdot 10^{+21}$	0.016	30.953	$2.466 \cdot 10^{+23}$	-0.016	333.447
R13	$CH_3(a) + OH(a) \rightleftharpoons CH_2(a) + H_2O(a)$	$2.014 \cdot 10^{+21}$	0.004	73.229	$1.175 \cdot 10^{+22}$	-0.004	116.851
R14	$CH_2(a) + OH(a) \rightleftharpoons CH_2OH(a) + (a)$	$3.420 \cdot 10^{+21}$	-0.004	12.581	$2.191 \cdot 10^{+22}$	0.004	180.219
R15	$CH_2OH(a) + (b) \rightleftharpoons CH_2O(a) + H(b)$	$1.917 \cdot 10^{+22}$	0.012	12.654	$3.348 \cdot 10^{+20}$	-0.012	57
R16	$CH_2O(a) + OH(a) \rightleftharpoons CHO(a) + H_2O(a)$	$5.608 \cdot 10^{+21}$	0.012	51.570	$2.119 \cdot 10^{+22}$	-0.012	19
R17	$CHO(a) + OH(a) \rightleftharpoons CO(a) + H_2O(a)$	$5.921 \cdot 10^{+22}$	0.008	65.968	$8.990 \cdot 10^{+21}$	-0.008	26
R18	$CH_3(a) + (b) \rightleftharpoons CH_2(a) + H(b)$	$1.827 \cdot 10^{+21}$	0.000	123.976	$5.137 \cdot 10^{+22}$	-0.000	16
R19	$CH_2(a) + (b) \rightleftharpoons CH_2(b) + (a)$	$1.257 \cdot 10^{+22}$	0.000	13.103	$2.797 \cdot 10^{+22}$	-0.000	19
R20	$CH_2(a) + (b) \rightleftharpoons CH(a) + H(b)$	$3.793 \cdot 10^{+22}$	0.008	112.541	$2.987 \cdot 10^{+22}$	-0.008	16
R21	$CH(a) + (b) \rightleftharpoons CHO(a) + vac(b)$	$2.103 \cdot 10^{+21}$	0.008	24.821	$1.218 \cdot 10^{+21}$	-0.008	21
R22	$CH_2(b) + (a) \rightleftharpoons CH_2O(a) + vac(b)$	$2.155 \cdot 10^{+22}$	0.008	91.222	$2.425 \cdot 10^{+20}$	-0.008	9.(
R23	$CH_2O(a) + (b) \rightleftharpoons CHO(a) + H(b)$	$3.274 \cdot 10^{+21}$	0.008	69.676	$5.962 \cdot 10^{+22}$	-0.008	20
R24	$CHO(a) + (b) \rightleftharpoons CO(a) + H(b)$	$1.088 \cdot 10^{+23}$	0.004	55.610	$7.956 \cdot 10^{+22}$	-0.004	25
R25	$CHO(a) + (b) \rightleftharpoons CHO(b) + (a)$	$2.746 \cdot 10^{+22}$	0.018	76.549	$6.754 \cdot 10^{+21}$	-0.018	10
R26	$CHO(b) + (a) \rightleftharpoons CO(b) + H(a)$	$2.732 \cdot 10^{+21}$	-0.002	141.937	$2.123 \cdot 10^{+21}$	0.002	26
R27	$CO(a) + (b) \rightleftharpoons (a) + CO(b)$	$1.313 \cdot 10^{+21}$	0.011	33.868	$2.212 \cdot 10^{+21}$	-0.011	16
R28	$CO(b) + (a) \rightleftharpoons CO_2(a) + vac(b)$	$1.410 \cdot 10^{+21}$	0.010	42.023	$9.554 \cdot 10^{+20}$	-0.010	78
R29	$H(b) + (a) \rightleftharpoons OH(a) + vac(b)$	$1.886 \cdot 10^{+22}$	0.000	137.8	$4.222 \cdot 10^{+21}$	0.000	27
R30	$O_2(a) + (a) \rightleftharpoons O(a) + O(a)$	$3.815 \cdot 10^{+22}$	0.005	174.961	$1.744 \cdot 10^{+21}$	-0.005	59
R31	$O(b) + (a) \rightleftharpoons O(a) + (b)$	$2.380 \cdot 10^{+22}$	0.027	116.625	$1.797 \cdot 10^{+21}$	-0.027	10
R32	$O(a) + vac(b) \rightleftharpoons (a) + (b)$	$8.012 \cdot 10^{+21}$	0.020	48.597	$1.387 \cdot 10^{+22}$	-0.020	25
R33	$O_2(a) + vac(b) \rightleftharpoons O(a) + (b)$	$1.196 \cdot 10^{+24}$	0.025	81.408	$9.469 \cdot 10^{+22}$	-0.025	16
R34	$H(b) + (a) \rightleftharpoons H(a) + (b)$	$6.133 \cdot 10^{+22}$	0.002	148.173	$9.505 \cdot 10^{+21}$	-0.002	11
R35	$CHO(b) + OH(a) \rightleftharpoons H_2O(a) + CO(b)$	$2.992 \cdot 10^{+22}$	0.001	2.168	$3.113 \cdot 10^{+22}$	-0.001	15
R36	$CHO(b) + (a) \rightleftharpoons HCOO(a) + vac(b)$	$3.658 \cdot 10^{+21}$	0.000	11.580	$1.210 \cdot 10^{+21}$	0.000	8.(
R37	$HCOO(a) + OH(a) \rightleftharpoons CO_2(a) + H_2O(a)$	$2.305 \cdot 10^{+23}$	0.011	183.191	$4.912 \cdot 10^{+23}$	-0.011	37
R38	$HCOO(a) + (b) \rightleftharpoons H(b) + CO_2(a)$	$1.681 \cdot 10^{+23}$	0.007	177.623	$1.726 \cdot 10^{+24}$	-0.007	36
R39[†]	$H_2O(a) + (b) \rightleftharpoons OH(a) + H(b)$	$3.659 \cdot 10^{+21}$	0.000	12.5	$1.763 \cdot 10^{+22}$	0.008	10





H. Stotz, L. Maier, A. Boubnov, A.T. Gremminger, J.-D. Grunwaldt, O. Deutschmann. Journal of Catalysis 370 (2019) 152-175.

Homogeneous oxidation of light alkanes in the exhaust of lean-burn gas engines promoted by NO_x



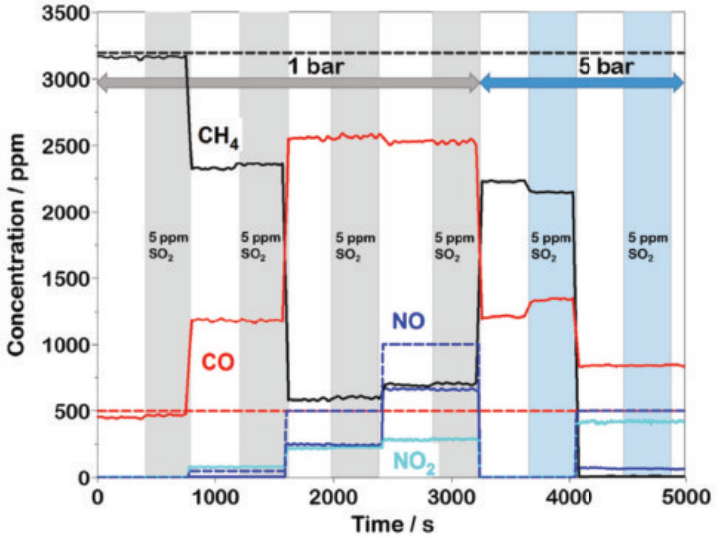
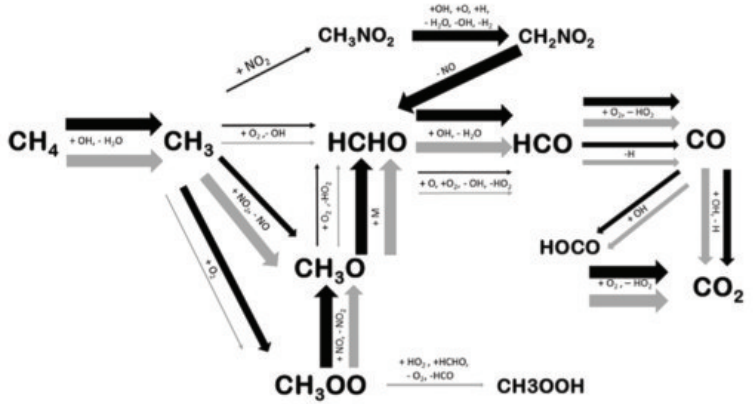


Fig. 14. Experimental result of methane oxidation in presence of 5 ppm SO_2. Inlet (dashed lines) and outlet (solid lines) concentration of CH_4, CO and NO_x as function of time at 650 °C for two different pressure (1 and 5 bar). Changes in inlet gas composition according to figure.



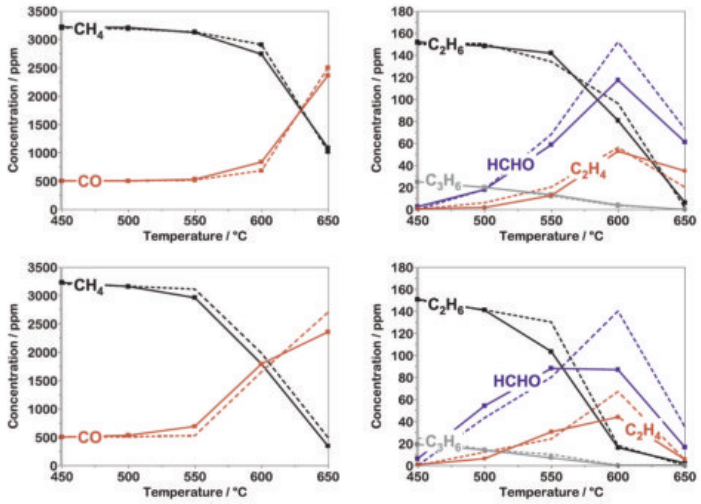
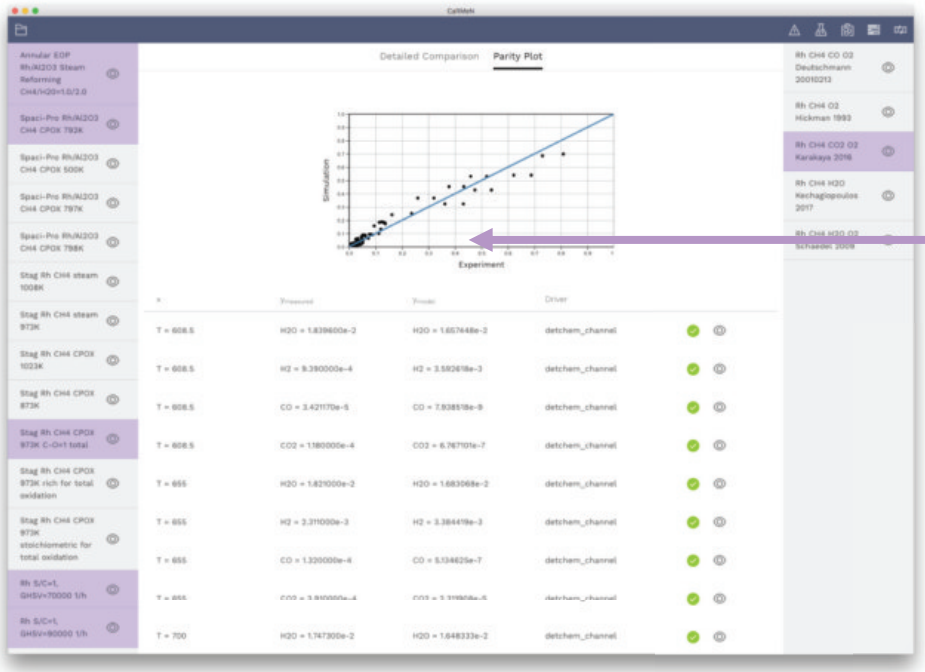


Fig. 4. Simulated (dashed lines) and measured (solid lines with squares) concentration profile of hydrocarbons and CO vs. temperature at *top*: 3 bar and *bottom*: 5 bar. Inlet gas composition GM1: 3200 ppm CH_4, 500 ppm CO, 150 ppm C_2H_6, 25 ppm C_3H_6, 120 ppm NO, 30 ppm NO_2, 10 vol% O_2 and 12 vol% H_2O in N_2. Mechanism of Konnov was used for calculation of concentration profiles.

B. Torkashvand, P. Lott, D. Zengel, L. Maier, J.-D. Grunwaldt, O. Deutschmann. Chem. Eng. J., doi.org/10.1016/j.cej.2018.08.186

Catalytic Reaction Mechanism Network (CaRMeN): A tool for archiving, analyzing and deriving kinetics



Combines chemical and physical models

Comparison of experimental and numerically simulated data



Experimental data for different reactors, conditions, groups for a given chemical system

H. Gossler, L. Maier, S. Angeli, S. Tischer, O. Deutschmann, PhysChemChemPhys 20 (2018) 10857.

www.detchem.de/carmen

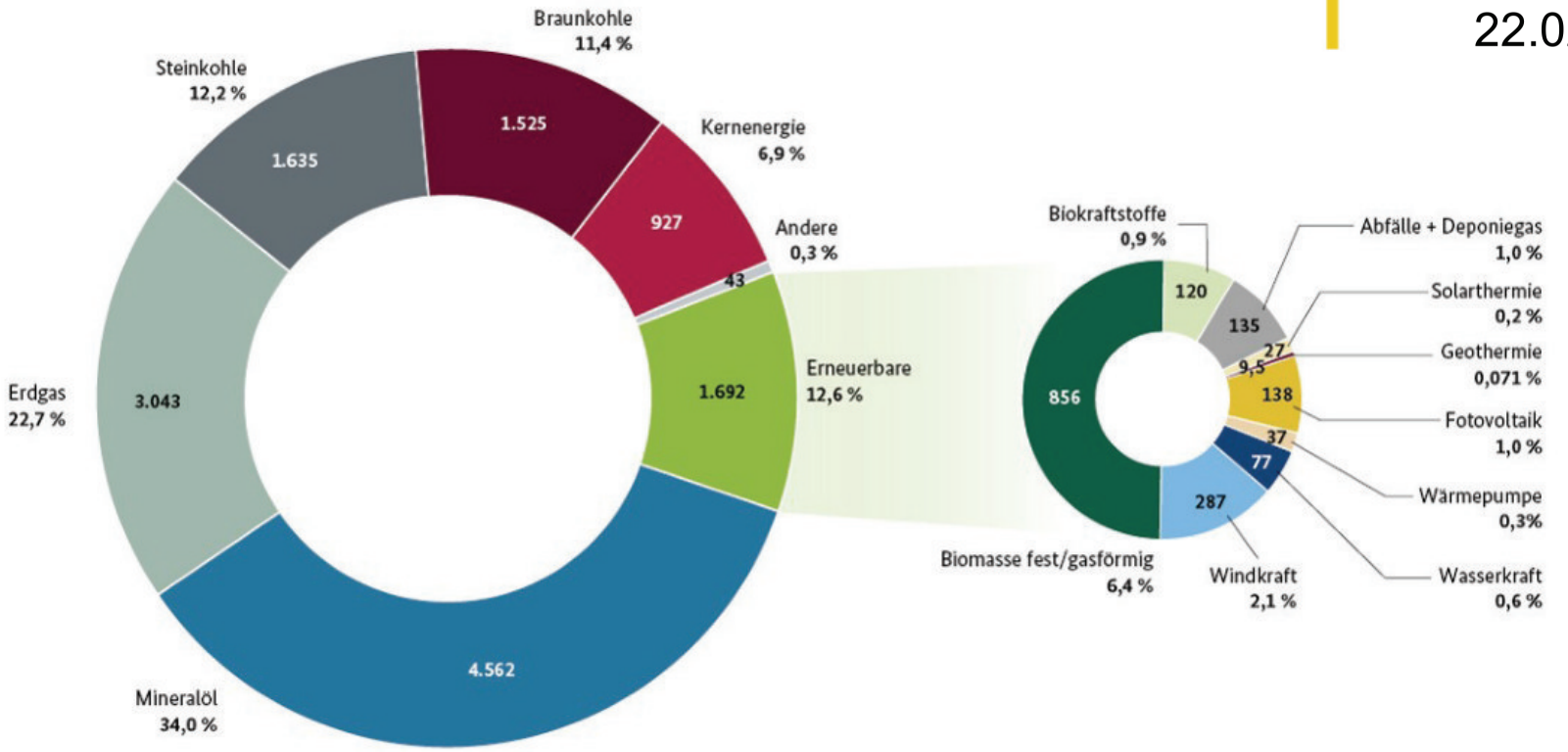
Emissionsreduzierung lokaler und globaler Schadstoffe: Forschungsresultate der Gruppe in 2018: Inhalt

- Stickoxidemissionen aus Diesel- und Gasmotoren
- Formaldehydemssionen aus Gasmotoren
- Methanemissionen
- **CO_2-Emissionen**
- Weitere Highlights

Status
Primary energy sources in Germany 2016

Bundesministerium für Wirtschaft und Energie

22.02.2017



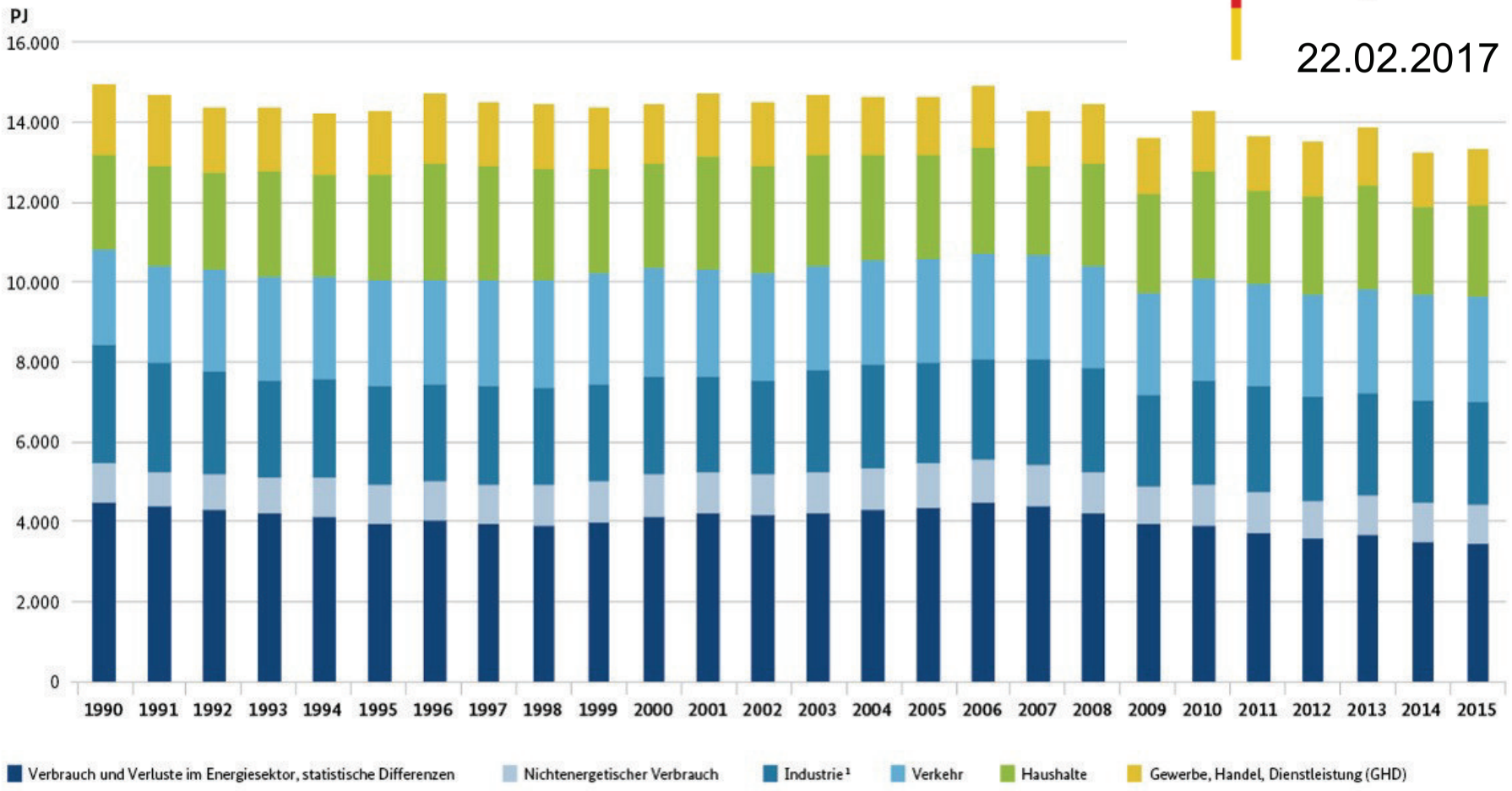
* Vorläufig

Status
Energy consuming sectors in Germany

Karlsruhe Institute of Technology

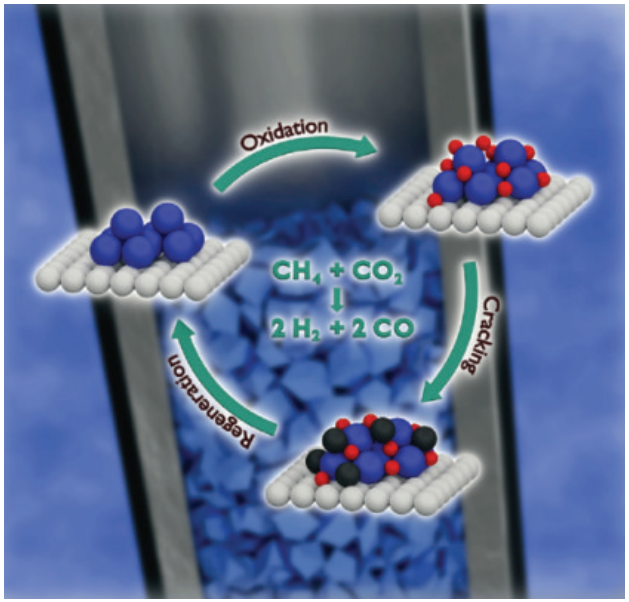
Bundesministerium für Wirtschaft und Energie

22.02.2017

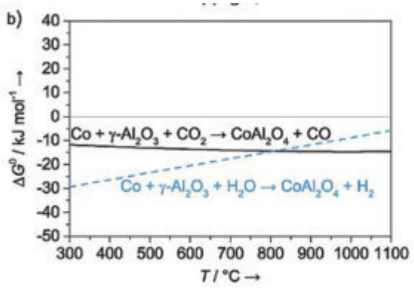


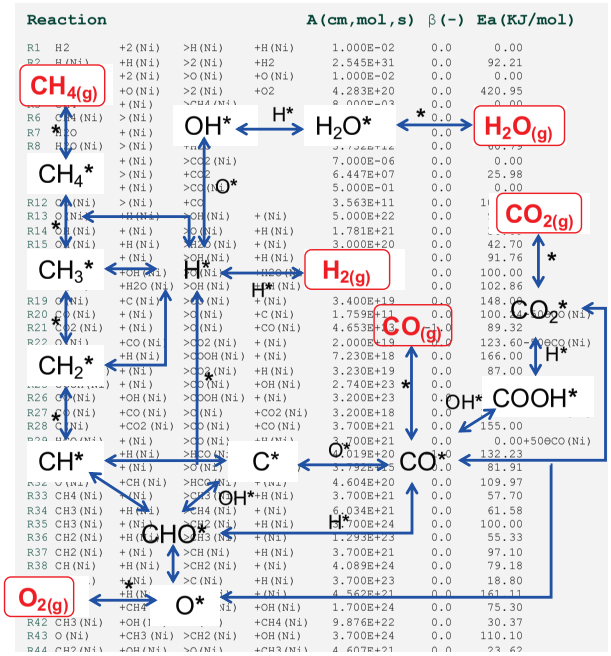
Microkinetic model for conversion of methane over Co-based catalysts: Temporal and spatial variation of catalyst state

- $CH_4 + CO_2 \rightarrow 2\ H_2 + 2\ CO$
- T > 950°C, p > 20 bar





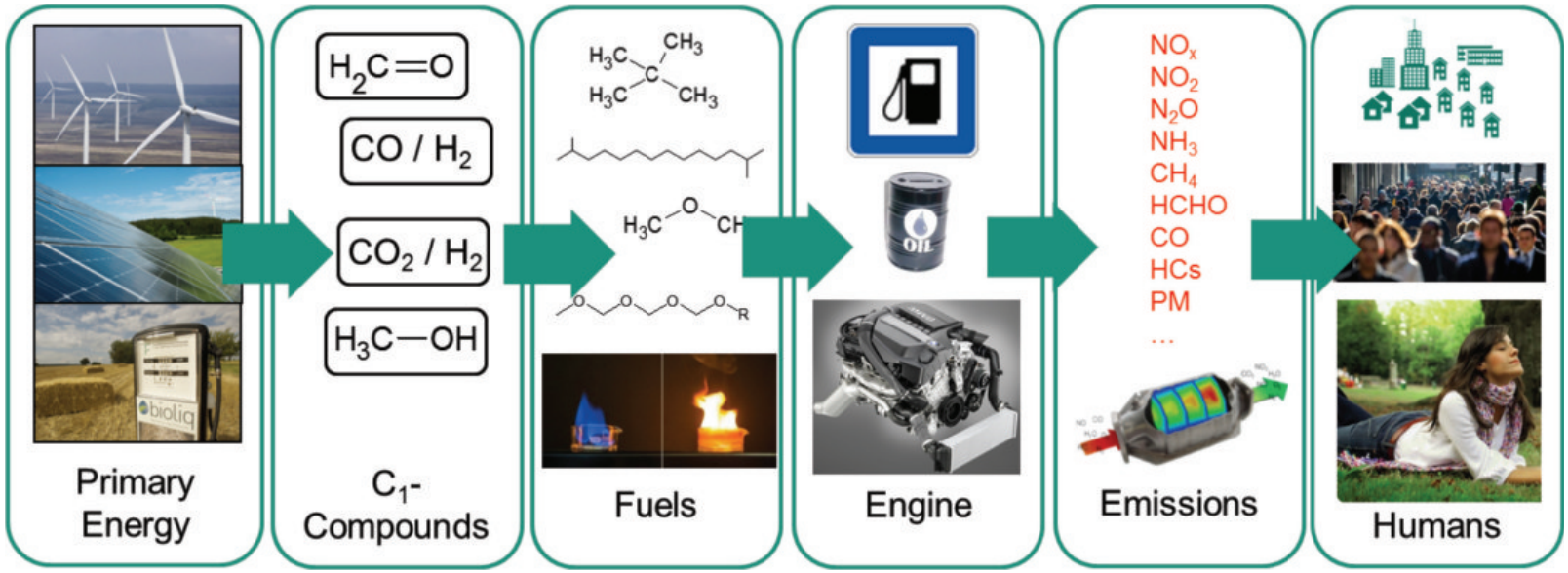






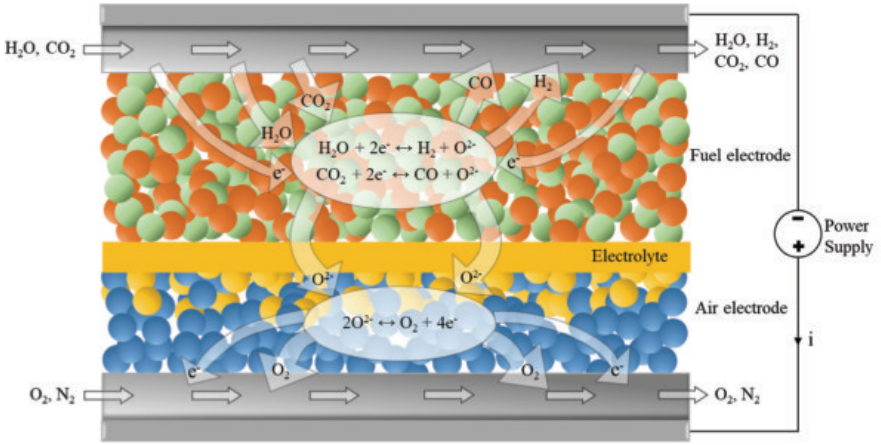
A. Giehr, L. Maier, S. Schunk, O. Deutschmann. ChemCatChem 10 (2018) 751.

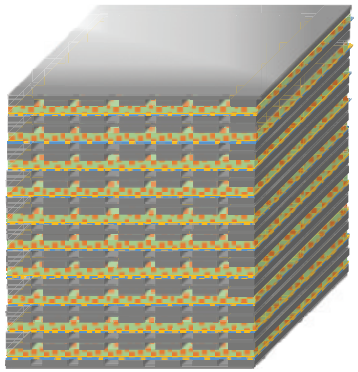
Sustainable route of energy, fuel and chemical production in the future

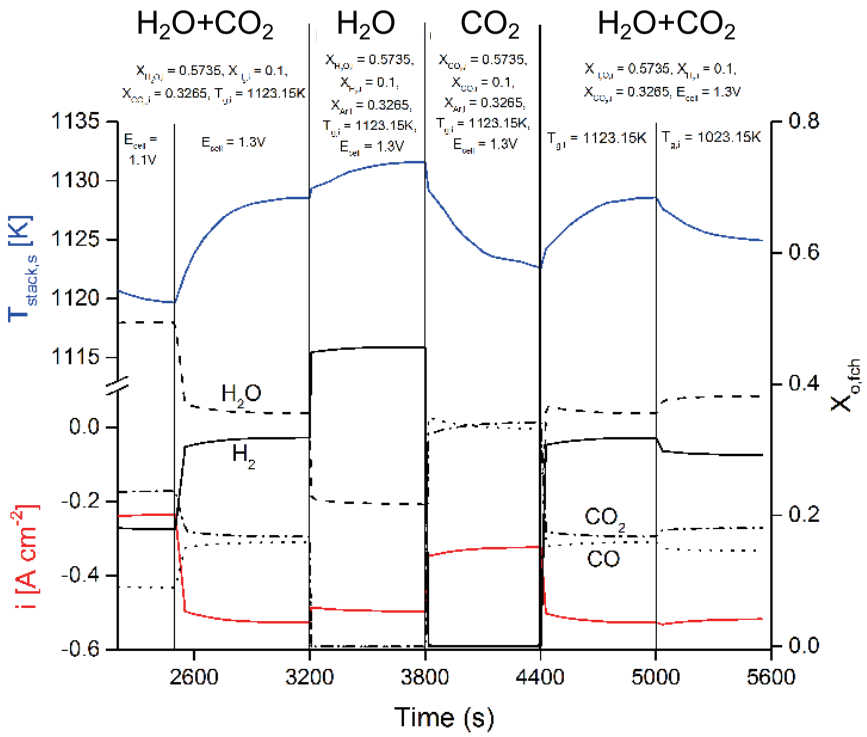


Solid oxide cells for co-electrolysis of H_2O/CO_2 for production of syngas (H_2/CO) from renewable sources

- Optimization of operating conditions depending on available electrical power and feed and on syngas-ratio demand

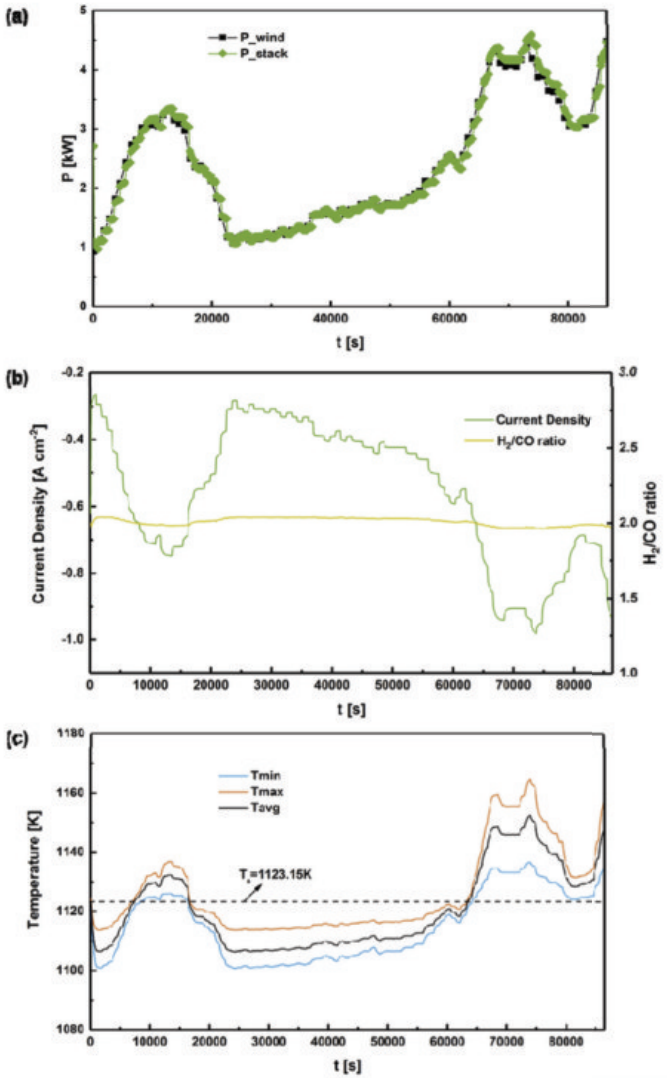




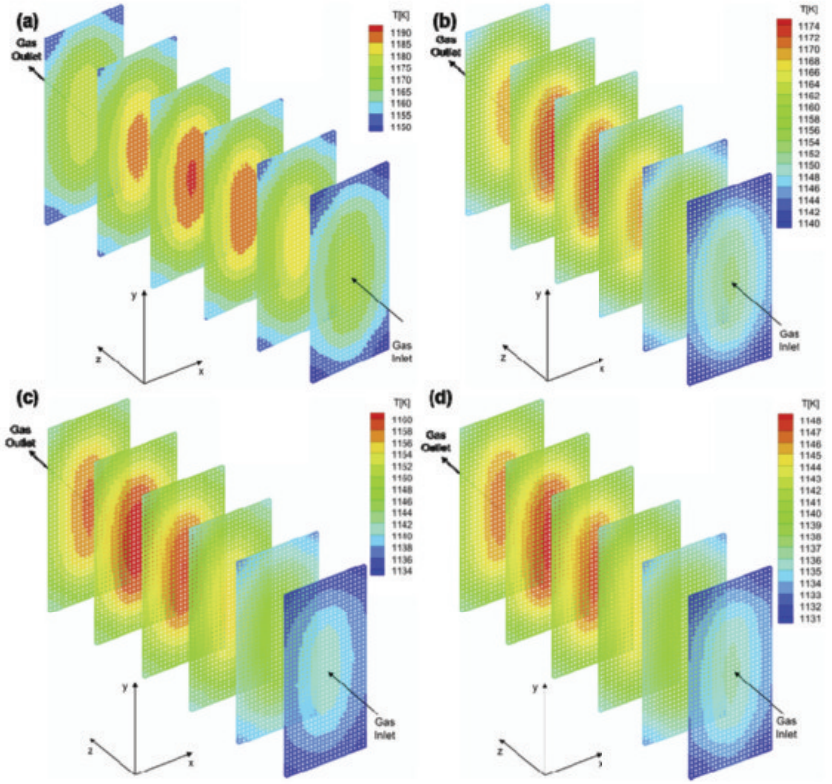


A. Bannerjee, Y. Wang, J. Diercks, O. Deutschmann. Appl. Energy 230 (2018) 996.

Dynamic behavior and control strategy study of CO_2/H_2O co-electrolysis in solid oxide electrolysis cells



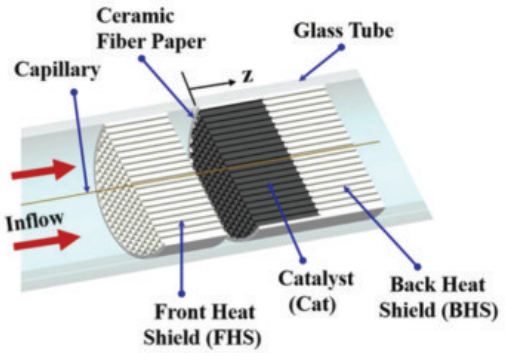
- Dynamic response of the (a) Power (b) Current density and H_2/CO ratio and (c) Temperature of the 40-cell F-design SOEC stack

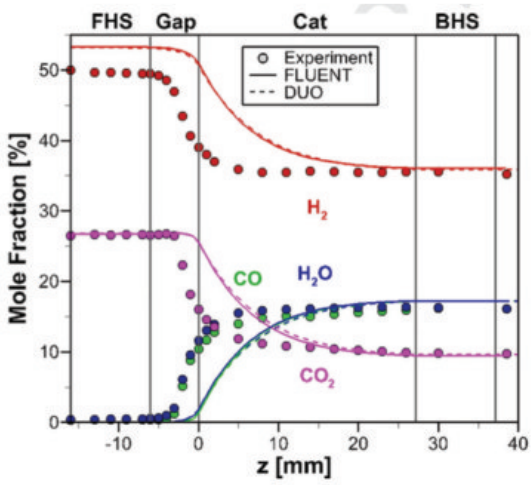


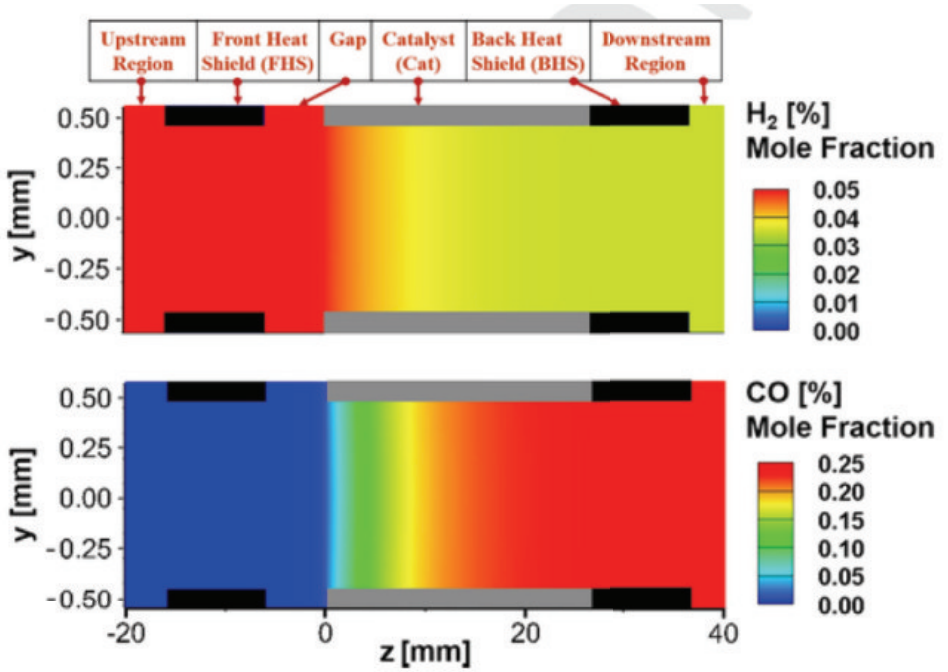
Y. Wang, A. Banerjee, O. Deutschmann. J. Power Sources 412 (2019) 255

Reverse Water Gas Shift (RWGS) over Ni - Spatially-Resolved Measurements and Simulations (code DUO)

- $H_2 + CO_2 = H_2O + CO$ used to establish H_2/CO ratio needed







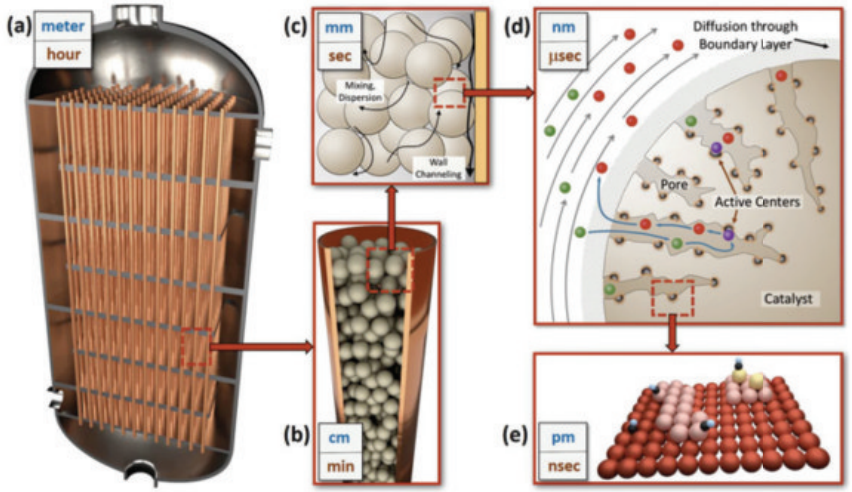
N. Benzinger, E. Daymo, M. Hettel, L. Maier, C. Antinori, P. Pfeifer, O. Deutschmann. Chem. Eng. J. (2019)
M. Hettel, E. Daymo, O. Deutschmann. Computers & Chemical Engineering 109 (2018) 166.

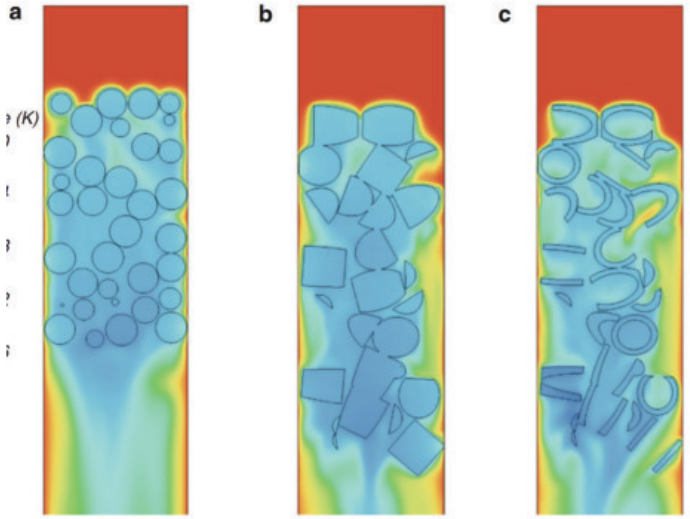
Emissionsreduzierung lokaler und globaler Schadstoffe: Forschungsresultate der Gruppe in 2018: Inhalt

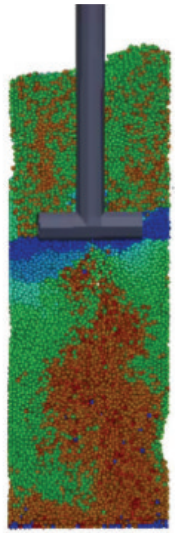
- Stickoxidemissionen aus Diesel- und Gasmotoren
- Formaldehydemssionen aus Gasmotoren
- Methanemissionen
- CO_2-Emissionen
- **Weitere Highlights**

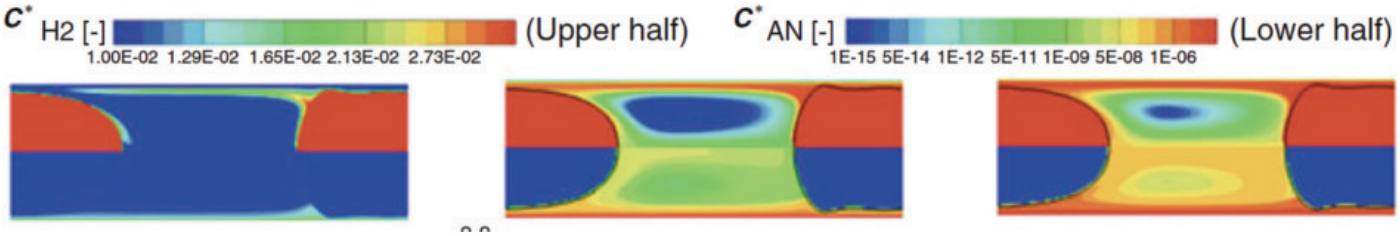
Computational Fluid Dynamics of Catalytic Reactors: Contribution to Handbook of Materials Modeling

Karlsruhe Institute of Technology



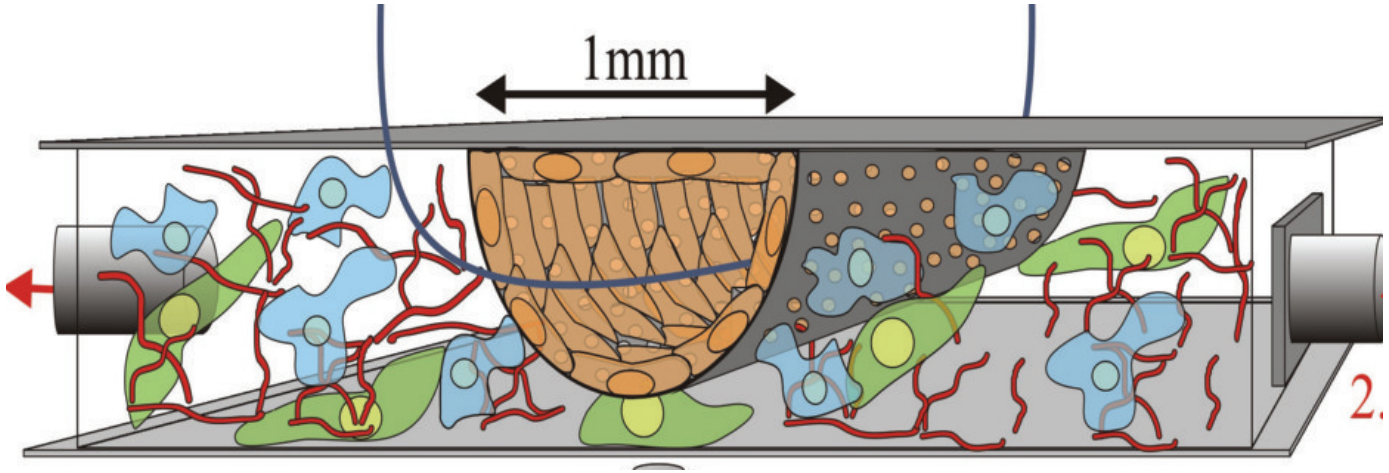


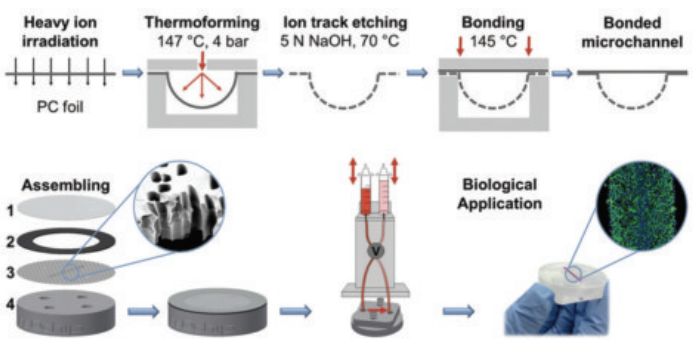


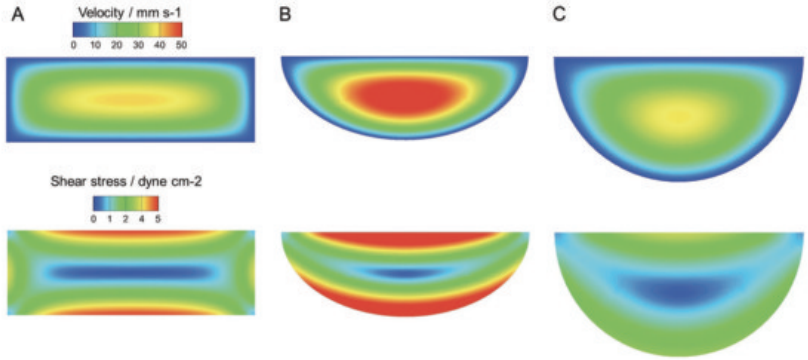


M. Hettel, M. Wörner, O. Deutschmann. Computational Fluid Dynamics of Catalytic Reactors. Chapter 6-1 in Handbook of Materials Modeling, W. Andreoni, S. Yip (eds.), Springer Nature 2018. https://doi.org/10.1007/978-3-319-50257-1_6-1

A Novel Microfluidic, Artificial Blood Vessel Scaffold for Vascularized 3D Tissues







V. Kappings, C. Grün, D. Ivannikov, I. Hebeiss, S. Kattge, I. Wendland, B.E. Rapp, M. Hettel, O. Deutschmann, U. Schepers. Advanced Materials Technologies (2018) 1700246.

High-temperature pressure reactor: Novel set-up to study conversion of CO_2 and pyrolysis at extreme conditions



S. Angeli, S. Lichtenberg, O. Deutschmann, 2018

High-temperature pressure reactor: Novel set-up to study conversion of CO_2 and pyrolysis at extreme conditions



S. Angeli, S. Lichtenberg, O. Deutschmann, 2018

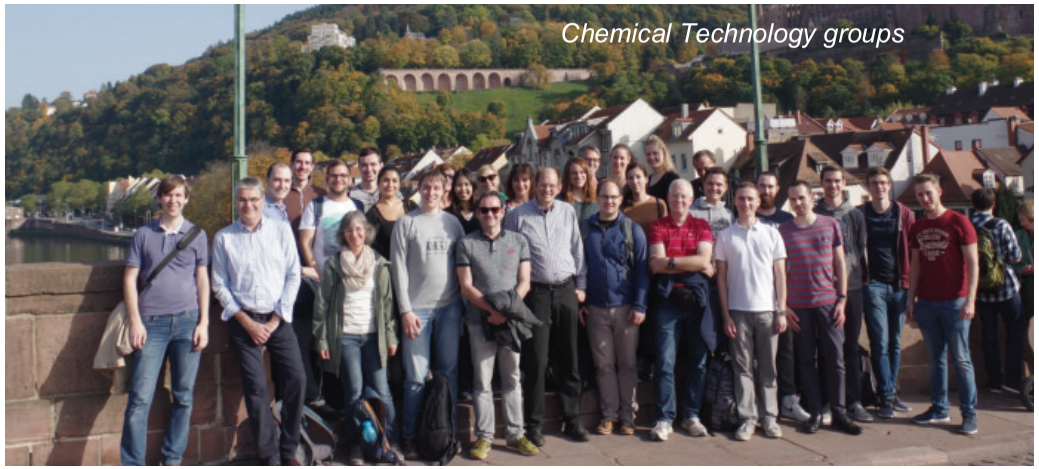
Emissionsreduzierung lokaler und globaler Schadstoffe: Forschungsresultate der Gruppe in 2018: Inhalt

- Stickoxidemissionen aus Diesel- und Gasmotoren
- Formaldehydemssionen aus Gasmotoren
- Methanemissionen
- CO_2-Emissionen
- **Weitere Highlights**

……. Sanierung 30.45



Acknowledgements



VT-Personal (U. Schwald, K. Schäfer
und viele andere)

Jan-Dierk Grunwaldt, Maria Casapu
und Mitarbeitern

Jörg Sauer, Stephan Pitter und
gesamten IKFT

Vielen Kollegen am KIT
und „around the world“

Collaboration

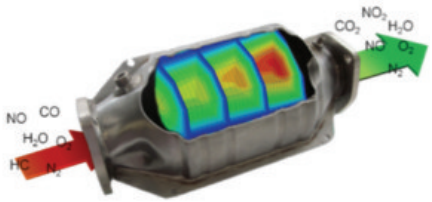
Financial support

Thank you for your attention!

Karlsruhe Institute of Technology

6th International Symposium on Modeling of Exhaust-Gas After-Treatment

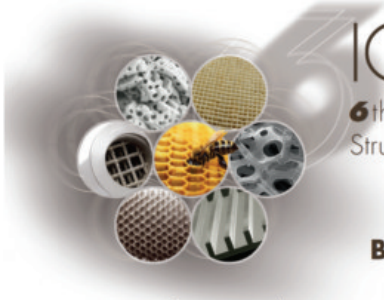
MODEGAT VI



September 8 - 10, 2019
Bad Herrenalb/Karlsruhe
Germany

1st circular (September 2018)

Email: symposium@modegat.org
Web: http://www.modegat.org



ICOSCAR6

6th International Conference on Structured Catalysts and Reactors

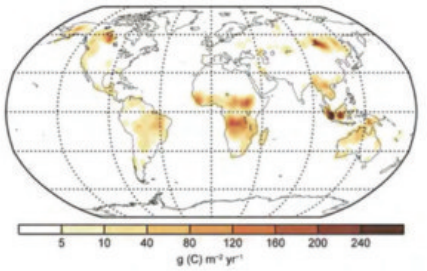
September 11–13, 2019
Bad Herrenalb · Germany

Abstract Submission Deadline: **January 15, 2019**

www.icoscar6.fau.de



SYMPOSIUM IM RAHMEN DER REIHE
›ZUKUNFTSFRAGEN DER GESELLSCHAFT‹



Luftschadstoffe:
Gesundheitsgefahren und technologische Lösungen
Ein wissenschaftlicher Diskurs

Freitag, 22. Februar 2019
15.00 bis 17.30 Uhr

Plenarsaal der
Akademie der Wissenschaften
und der Literatur
Geschwister-Scholl-Straße 2
55131 Mainz